PERFORMANCE OF AN OSWATISCH INLET WITH HEMISPHERICAL CENTERBODY AT ZERO ANGLE ATTACK

John Francis Moran

NPS67-81-009

NAVAL POSTGRADUATE SCHOOL

Monterey, California

THESIS

PERFORMANCE OF AN OSWATISCH INLET WITH HEMISPHERICAL CENTERBODY AT ZERO ANGLE OF ATTACK

by

John Francis Moran

June 1981

Thesis Advisor: A. E. Fuhs

Prepared for: Defense Advanced Research Projects Agency
1400 Wilson Boulevard
Arlington, VA 22209

NAVAL POSTGRADUATE SCHOOL
Monterey, California 93940

Rear Admiral J. J. Ekelund
Superintendent

David Schrady
Acting Provost

This thesis prepared in conjunction with research supported in part by the Defense Advanced Research Projects Agency.

REPORT DOCUMENTATION PAGE		READ INSTRUCTIONS BEFORE COMPLETING FORM
1. REPORT NUMBER NPS67-81-009	2. GOVT ACCESSION NO.	3. RECIPIENT'S CATALOG NUMBER
4. TITLE (and Subtitle) Performance of An Oswatisch Inlet With Hemispherical Centerbody at Zero Angle of Attack		5. TYPE OF REPORT & PERIOD COVERED Master's Thesis; June 1981
		6. PERFORMING ORG. REPORT NUMBER NPS67-81-009
7. AUTHOR(s) John Francis Moran		8. CONTRACT OR GRANT NUMBER(s) ARPA Order No. 4035
9. PERFORMING ORGANIZATION NAME AND ADDRESS Naval Postgraduate School Monterey, California 93940		10. PROGRAM ELEMENT, PROJECT, TASK AREA & WORK UNIT NUMBERS Program Code No. OG10/ 1G10 Program Element No. 62702E
11. CONTROLLING OFFICE NAME AND ADDRESS Naval Postgraduate School Monterey, California 93940		12. REPORT DATE June 1981
		13. NUMBER OF PAGES 86
14. MONITORING AGENCY NAME & ADDRESS (if different from Controlling Office) Defense Advanced Research Projects Agency 1400 Wilson Blvd Arlington, VA 22209		15. SECURITY CLASS. (of this report) UNCLASSIFIED
		15a. DECLASSIFICATION/DOWNGRADING SCHEDULE

16. DISTRIBUTION STATEMENT (of this Report)

Approved for public release; distribution unlimited

17. DISTRIBUTION STATEMENT (of the abstract entered in Block 20, if different from Report)

18. SUPPLEMENTARY NOTES

19. KEY WORDS (Continue on reverse side if necessary and identify by block number)

Guided Projectiles; Precision Guided Munitions; Guns; Gun Launched Ramjet; Ramjet Performance; Semi Active Laser Guided Projectile

20. ABSTRACT (Continue on reverse side if necessary and identify by block number)

This thesis analyzes the performance of a ramjet with an Oswatisch inlet using a blunt centerbody and compares performance to a baseline ramjet using an inlet with a conical spike at Mach 3.0.

Inlet performance as a ratio of inlet lip to nose centerbody ratio, r_L/r_n, is developed. The capture streamline for each ratio is determined and the coefficient of additive drag is calculated as a function of r_L/r_n. Setting thrust coefficient equal to

DD FORM 1 JAN 73 1473 EDITION OF 1 NOV 65 IS OBSOLETE
(Page 1) S/N 0102-014-6601

coefficient of drag, the performance of two ramjets is determined. One ramjet is the baseline with a spike inlet; the other ramjet uses the blunt centerbody.

Ramjets and inlets are compared on the basis of specific fuel consumption, excess thrust coefficient and specific thrust. For the ramjet with blunt centerbody, performance parameters were calculated as a function of inlet lip radius to nose centerbody radius. Also compared is the effect of the ratio, r_L/r_n, on relative detection range. For both types of ramjets, the detection range is reduced by approximately 66%. Performance of the ramjet with blunt nosed centerbody is severly handicapped due to high additive drag and poor pressure recovery. Specific fuel consumption is approximately 50% greater for the ramjet with the blunt centerbody compared to the ramjet with the spike inlet.

Performance Of An Oswatisch Inlet With Hemispherical Centerbody At Zero Angle Of Attack

by

John Francis Moran
Lieutenant, United States Navy
B.S., United States Naval Academy, 1975

Submitted in partial fulfillment of the
requirements for the degree of

MASTER OF SCIENCE IN ENGINEERING SCIENCE

from the

NAVAL POSTGRADUATE SCHOOL
June 1981

ABSTRACT

This thesis analyzes the performance of a ramjet with an Oswatisch inlet using a blunt centerbody and compares performance to a baseline ramjet using an inlet with a conical spike at Mach 3.0.

Inlet performance as a ratio of inlet lip to nose centerbody ratio, r_L/r_n, is developed. The capture streamline for each ratio is determined and the coefficient of additive drag is calculated as a function of r_L/r_n. Setting thrust coefficient equal to coefficient of drag, the performance of two ramjets is determined. One ramjet is the baseline with a spike inlet; the other ramjet uses the blunt centerbody.

Ramjets and inlets are compared on the basis of specific fuel consumption, excess thrust coefficient and specific thrust. For the ramjet with blunt centerbody, performance parameters were calculated as a function of inlet lip radius to nose centerbody radius. Also compared is the effect of the ratio, r_L/r_n, on relative detection range. For both types of ramjets, the detection range is reduced by approximately 66%. Performance of the ramjet with blunt nosed centerbody is severly handicapped due to high additive drag and poor pressure recovery. Specific fuel consumption is approximately 50% greater for the ramjet with the blunt centerbody compared to the ramjet with the spike inlet.

TABLE OF CONTENTS

I. INTRODUCTION------------------------------------ 15

A. BACKGROUND---------------------------------- 15

B. PURPOSE------------------------------------- 19

II. FORMULATION OF INLET PERFORMANCE EQUATIONS AND INLET FLOW FIELD---------------------------- 21

A. INLET DESIGN OPTIONS------------------------ 21

B. CALCULATION OF STAGNATION PRESSURE RATIO OF THE INLET-------------------------------- 23

C. FLOW FIELD DESCRIPTION IN THE VICINITY OF A BLUNT NOSE----------------------------- 32

III. CALCULATION OF RAMJET PERFORMANCE--------------- 51

A. PERFORMANCE EQUATIONS----------------------- 51

IV. DISCUSSION OF RESULTS-------------------------- 56

A. PERFORMANCE CRITERION---------------------- 56

B. RESULTS OF CALCULATIONS-------------------- 58

V. CONCLUSIONS------------------------------------- 69

APPENDIX A - NASA Ames COMPUTER PROGRAM DESCRIPTION--- 70

APPENDIX B - MASS CONTINUITY METHOD OF DETERMINING STREAMLINE SHAPE------------------------ 74

APPENDIX C - ADDITIVE DRAG COMPUTATION--------------- 80

LIST OF REFERENCES-------------------------------- 84

INITIAL DISTRIBUTION LIST------------------------- 85

LIST OF FIGURES

I-1 U.S. Navy 5"/54 Semi Active Laser Guided Projectile (SALGP) ---------- 17

II-1 Supersonic Inlet With Blunt Centerbody ------- 24

II-2 Supersonic Inlet With Conical Spike ---------- 24

II-3 Supersonic Inlet (variation) ----------------- 25

II-4 Supersonic Inlet With Isentropic Spike ------- 25

II-5 Cylindrical Analog Of Busemann Biplane Inlet - 26

II-6 Flow Regions Around A Blunt Nosed Body ------- 27

II-7 Magnitude Of Pressure Losses ---------------- 29

II-8 Identification Of Locations For Description Of Pressure Recovery Losses In A Conical Inlet ---------- 30

II-9 Flow Geometry Around The Blunt Nose Showing Bow Shock, Streamtube And Body Locations ----- 34

II-10 Magnified View Of Geometry Between Points 1 And 2 Of Figure II-9 ---------- 38

II-11 Geometry To Determine Component Of Velocity Normal To The Area For Integration Of Mass Flux ---------- 39

II-12 Flow Field Geometry For The Angular Method Of Streamtube Determination ---------- 44

II-13 Geometry For Additive Drag Calculation ------- 46

II-14 Geometry Of Streamtubes At The Inlet Annulus Used To Calculate Average Stagnation Pressure, π_d' ---------- 50

IV-1 Combustor Exit Temperature As A Function Of r_L/r_n At $C_f = C_D = 0.349$ ---------- 59

IV-2 Excess Thrust Coefficient As A Function Of r_L/r_n ---------- 60

IV-3 Specific Fuel Consumption As A Function Of r_L/r_n For Ramjet With Blunt Centerbody ---- 61

IV-4 Relative Detection Range As A Function Of r_L/r_n ---------- 63

IV-5 Mass Flow Ratio And Capture Radius Ratio As A Function Of r_L/r_n ---------- 64

IV-6 Additive Drag Coefficient As A Function Of r_L/r_n For An Inlet At The Shoulder (Z=1.00) ---------- 65

IV-7 Bow Shock Wave And Capture Streamtube For r_L/r_n Equal To 1.1 And 1.4 ---------- 66

A-1 Angular Relationship At The Shock Front For δ, β, θ ---------- 73

LIST OF TABLES

II-1 Capture Radius, r_s, As A Function Of Lip Radius, r_L, For r_n Equal To 1.0 Inch At Body Station $Z = 1.00$ -------------------- 36

II-2 Summary Of Radius Of Capture Streamtube, Additive Drag Coefficient, And Mass Flow Ratio -- 48

IV-1 Comparison Of Spike Inlet Versus Two Blunt Nose Inlets -- 68

A-1 Reference Values For OGIVE and IMPLCBO Programs --- 72

B-1 Variables For Capture Streamtube Computer Program -- 75

B-2 Capture Streamtube Program Listing ---------- 77

C-1 Variables For Coefficient Of Additive Drag Computer Program ------------------------- 81

C-2 Coefficient Of Additive Drag Program Listing -- 82

LIST OF SYMBOLS

Symbol	Explanation	Units
a	Speed of sound	ft/sec
A	Area (with subscript)	ft^2
A_r	Reference area which is maximum cross sectional area for projectile	ft^2
C_{dad}	Coefficient of additive drag	
C_p	Coefficient of specific heat capacity at constant pressure	$BTU/lb_m{}^\circ R$
C_f	Coefficient of thrust	
C_D	Coefficient of airframe drag	
C_{fe}	Coefficient of excess thrust	
D_a	Additive drag	
f	Fuel air ratio ($\dot{m}_f/\dot{m}_o$)	
F	Thrust	lbf
g	Gravitational constant	ft/sec
h	Heating value of hydrocarbon	BTU/lb_m
$\dot{m}$	Mass flow rate	slug/sec or lb_m/sec
$\dot{m}_s$	Mass flow rate in the capture streamtube at the bow shock	lb_m/sec
$\dot{m}_s^\circ$	Mass flow rate (reference) equal to mass flow rate in a circular streamtube of radius r_L	lb_m/sec
p	Pressure (static without subscript)	lb/ft^2
Q	Non dimensional free stream velocity defined as u_s/v_m	

Symbol	Explanation	Units
q_o	Free stream dynamic pressure	lb_f/ft^2
r_n	Nose radius of inlet centerbody; nose radius of seeker	in
r_s	Radius of the capture streamline at the intersection with the bow shock wave	in
r_L	Outer radius of the inlet annulus	in
R	Distance normal to projectile axis for region 2 coordinate system	in
r	Distance from projectile axis using cylindrical coordinates; r is identical to Y used in the computer printout	in
S	Capture streamtube area	ft^2
SF	Specific thrust	$lb_f/(lb_m/sec)$
SFC	Specific fuel consumption	$(lb_m/hr)/lb_f$
S_r	Quantity defined by equation 44	
T	Temperature	°R
u	Component of velocity in the Z or X direction	ft/sec
v_m	Maximum velocity obtained when a gas with stagnation speed of sound (a_t) is expanded into a vacuum; $v_m=(2/(\gamma-1))^{1/2}\ a_t$	ft/sec
v	Component of velocity normal to projectile axis in region 1; for ramjet performance	
v_o	Velocity of air at designated station of ramjet	ft/sec
x	Ratio as defined in equation 30	
X	Distance parallel to projectile axis for region 1 coordinate system	in

Symbol	Explanation	Units
Z	Distance parallel to projectile axis for region 2 coordinate system	in
Y	Distance perpendicular to projectile axis for region 1 coordinate system	in
α	Angle of attack	degrees
β	Angle measured from reference direction to the local velocity flow vector	
γ	Ratio of heat capacities	
η	Efficiency	
θ	Angle of streamtube between two data points	degrees
π	Ratio of downstream stagnation pressure to upstream stagnation pressure (with subscript); Ratio of circle circumference to circle diameter (without subscript)	
ρ	Density	lb_m/ft^2

Subscripts

a	Additive drag
b	Burner
d	Diffuser
e	Exit station of ramjet engine
f	Force (with lb)
i	Integer identifying points along capture streamline
j	Integer identifying individual streamtubes within the capture streamline
L	Lip of inlet annulus
m	Mass (with lb)
n	Normal to surface; nozzle with ramjet; nose of projectile
o	Inlet station of ramjet engine
s	Free stream values at the bow shock on the upstream side
t	Stagnation values
1	Designates values from region 1 as defined in Figure II-6
2	Designates values from region 2 as defined in Figure II-6
3	Combustor exit station
α	Values along a constant line as indicated in Figure II-9
∞	Free stream values

Superscripts

$(\ )'$	Values tabulated in NASA Ames computer printout (non dimensional)
$(\bar{\ })$	Average value

ACKNOWLEDGMENT

The author wishes to express his thanks to Dr. Paul Kutler and Dr. Dennis Chausse of NASA Ames Computational Fluid Dynamics Branch for their assistance in the calculation of the flow field over the blunt noses body. Their assistance aided this work immeasurably.

Also, the author wishes to express his deepest gratitude to Dr. Allen E. Fuhs for his patience, guidance and time. Without him, this thesis would not have been possible.

I. INTRODUCTION

A. BACKGROUND

The rapid development and operational deployment of long range antiship cruise missiles has generated demanding requirements for the anti-ship missile defense (ASMD) mission. The threat has necessitated that the Navy develop the concept of a "defense in depth" for the defensive doctrine of a carrier battle group (CBG). The doctrine emphasizes the utilization of all available weapon systems in a layered defense to defeat hostile targets. Conceivably, an anti-ship missile (ASM) could survive attacks from extremely long range missiles, the E-2C and F-14 combat air patrol (CAP) team, Standard ER and Standard MR missiles, conventional gun ordnance, point defense weapons and close in defense weapons, such as Phalanx, prior to reaching a high value unit. Since enemy doctrine is to fire the ASM in such numbers as to overwhelm the Command and Control capability of the CBG and of an individual vessel, the accent of new ASMD weapons systems is on quick response time, short time of flight and a high degree of accuracy against a manuvering ASM.

Although a single saturation raid could possibly be defeated, what about a second or third raid in a single day? Will the CBG have enough missiles to supplement airborne CAP

and still destroy the ASM threat 30 to 40 miles from the high value unit?

One solution to this vexing problem is to modify the 5"/54 Semi-Active Laser Guided Projectile (SALGP) which is illustrated in Figure I-1. The SALGP round is currently undergoing operational evaluation (OPEVAL) prior to fleet wide introduction [Ref. 1] and consists of a five inch projectile with a laser seeker on the projectile nose. The round is designed to "home in" on laser energy reflected from a target by a laser illuminator. The modification to the SALGP round consists of replacing the laser seeker head with an infrared (IR) seeker and adding a solid fuel ramjet to power the projectile. The ramjet would provide constant speed over a longer portion of the flight path and provide energy in the terminal phase of flight to allow for manuvering to hit a manuvering target. The modified SALGP is identified as a gun launched missile (GLM). The modifications would allow the GLM to become a fire and forget round requiring no terminal guidance from the ship.

Although not helping in the long range defense of a CBG, the GLM would complement the point defense and close in defense weapon systems to the ships in the U.S. Navy today.

The GLM will allow a naval vessel without a missile system and with a properly configured gun system to increase its anti-air warfare (AAW) capability in a cost effective

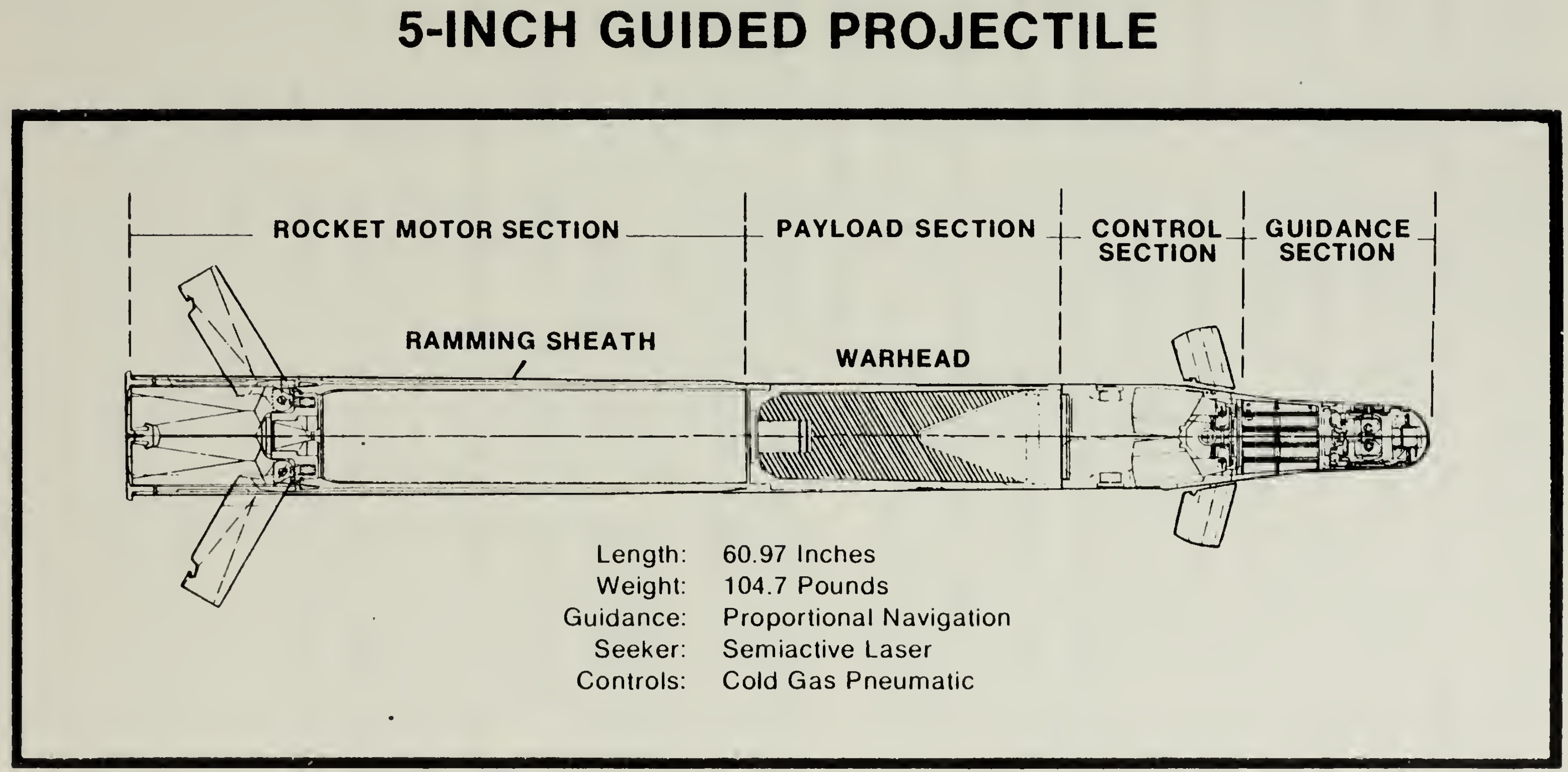

Figure I-1 U.S. Navy 5"/54 Semi Active Laser Guided Projectile (SALGP)

[illegible]

way. More GLM rounds can be carried in existing gun magazines than missile rounds can be carried in current missile magazines. Within a ten nautical mile zone around a ship, the GLM will have a faster response time, a shorter time of flight and be as accurate as guided missiles in the current Navy inventory. Fast response and short time of flight are due to the initial velocity imparted to the GLM by the 5"/54 gun. The shape of the nose of the GLM round will be constrained by the use of the hemispherical lense surface for the infrared seeker in the projectile nose. This blunt nose, although optimized for the sensor optics, is not necessarily the best aerodynamic shape.

Although the SALGP has the potential to be highly effective in the Naval Gunfire Support (NGFS) and in the Surface to Surface Warfare (SUW) missions, it was not designed initially for the Air Warfare (AAW) or Anti-ship Missile Defense (ASMD) missions. Consider a GLM based on SALGP hardware to the maximum extent possible. To become successful in the AAW/ASMD mission areas, it is essential to improve the overall SALGP performance and capability. One area to achieve easily measured performance gains is in the method of propelling the SALGP.

One propulsion proposal that decreases mission flight time and increases mission effectiveness is to replace the solid propellant rocket on the SALGP round with that of a

ramjet with either liquid or solid fuel. Obviously, to keep total system developement and procurement costs low, and therefore warrant the use of a ramjet in a cost effective analysis, the SALGP round should be changed as little as possible in adding the ramjet. Effectively, the designer is constrained to use a blunt nosed centerbody to house the IR seeker and sensor package. The remainder of the projectile is constrained by the dimensions of the handling equipment in the MK 45 mount and Department of the Navy Specifications [Ref. 2].

B. PURPOSE

One purpose of this thesis is to investigate the effect that a blunt nosed centerbody has on the pressure recovery of an inlet. The pressure recovery is an important indicator of ramjet performance, for poor pressure recovery will reduce the flight envelope over which the ramjet operates.

Although drag is large, the blunt nosed body was aerodynamically feasible for a rocket guided projectile, since the operation of the rocket engine does not require air to be "brought onboard". The use of a ramjet may prove inadviseable or infeasible due to aerodynamics of the flow around the blunt nose body enroute to the inlet annulus. The pressure recovery, or lack of, may also require the body shape surrounding the IR sensor system be reconfigured, within existing system constraints, to allow for ramjet operation.

The aerodynamic model used was that of a hemispherical body with an attached cylindrical body of constant diameter. The flow was calculated for a cylinder length equal to four times the nose radius. Distances involved were normalized to the nose radius, r_n. This is the same as the radius of the hemisphere.

The National Aeronautics and Space Administration Ames Research Center (NASA Ames) calculated the flow over a hemispherical body with an attached cylinder over the range of Mach numbers from 1.8 to 3.4, in steps of 0.2, at zero angle of attack and at Mach 3.4 with an angle of attack (α) equal to 10 degrees. The calculations provide flow field data which included shock shape, sonic line, velocity components, pressure, density, entropy and similar flow parameters. The calculations were done by computer code contained in two separate programs. For a further discussion of the programs and the various inputs see Appendix A.

Section II reports on inlet performance and the inlet flow field. Section III reports on ramjet performance for a blunt nosed centerbody for the inlet and compares the performance of a ramjet with an isentropic spike inlet.

II. FORMULATION OF INLET PERFORMANCE EQUATIONS AND INLET FLOW FIELD

A. INLET DESIGN OPTIONS

In developing a quantitative basis for comparison of various inlet designs, several items of information are needed.

First, information needed is the drag at the different Mach numbers and a correlation of drag versus Mach number. The blunt nosed centerbody produces a detached shock that stands off a distance from the body. A conical inlet produces an attached oblique shock.

Second, the on-design performance of the inlet design must be evaluated. In particular, the pressure recovery of the inlet is important. What happens to this recovery ratio when the position of the annulus is moved axially along the body? If the location is fixed and the radius of the inlet lip varied what happens to the inlet performance? A comparison must be made of the relative ranges attained by a ramjet with an isentropic spike and one with a blunt nosed centerbody must be made. Also of concern is how sensitive the ramjet performance is to angle of attack variations.

Third, off-design performance of the ramjet is of interest in several aspects. First, how does the pressure recovery of the inlet vary at different Mach numbers? Ramjet performance is sensitive to the inlet pressure recovery. Generally

ramjet performance tends to improve initially at higher Mach numbers. Second, how does this affect projectile drag and what effect, if any, is transmitted to the projectile range? Third, what is the operational region over which the inlet and ramjet will continue to operate? The lower performance limit of the inlet is that Mach number where the normal shock within the inlet is expelled. This condition is refered to as subcritical ramjet operation and can lead to a condition called "buzz". The upper performance limit of the inlet is the maximum flight speed at which adequate pressure recovery can be attained. Last, how does the angle of attack affect off design performance?

The desire that the ramjet powered GLM fit within the existing confines of the 5"/54 MK 45 gun limits the inlet design to that of the axisymmetric variety. In theory, "pop-up" inlets or scoops could be used. However, the ability of the inlets to survive a gun launch of 8000 g's and function reliably increases the complexity of the round; variable geometry inlets are not a good use of the remaining available space in the projectile. The small diameter of the projectile, coupled with the nose mounted laser seeker, requires intelligent use of available space.

The axisymmetric inlets which could be utilized are 1) blunt nosed centerbody, 2) conical nose and variations, 3) an unconstrained design, an isentropic spike for example, and 4) a cylindrical analog of the Busemann Biplane.

The blunt nose shown in Figure II-1 is currently in use on the SALGP projectile, without the annulus. As modeled by the simulation, the inlet consists of a hemispherical nose connected to a constant diameter body extending beyond the inlet lip. The conical nose in Figure II-2 uses a cone of fixed angle to focus the shock wave at the inlet lip when at the design Mach number. A variation is shown in Figure II-3. Shown in Figure II-4 is the unconstrained design. The design would consist of an isentropic spike. Figure II-5 shows the cylindrical analog of the Busemann Biplane. The inlet "swallows" the oblique shock wave formed by the nose at the design Mach number and has a body of constant diameter. The advantage is the elimination of external wave drag.

B. CALCULATION OF STAGNATION PRESSURE RATIO OF THE INLET

For calculation purposes, the flow around the blunt nosed body is divided into two segments as shown in Figure II-6. Region 1 is the region of flow from upstream infinity to the shoulder of the centerbody. The centerbody shoulder is located in plane S in Figure II-6. Region 1 is characterized by flow in both the longitudinal and radial directions. Region 2 is the region of flow downstream of plane S. The majority of the flow is in the longitudinal direction with a relatively small radial component. The origin for coordinate systems for regions 1 and 2 is the same as illustrated

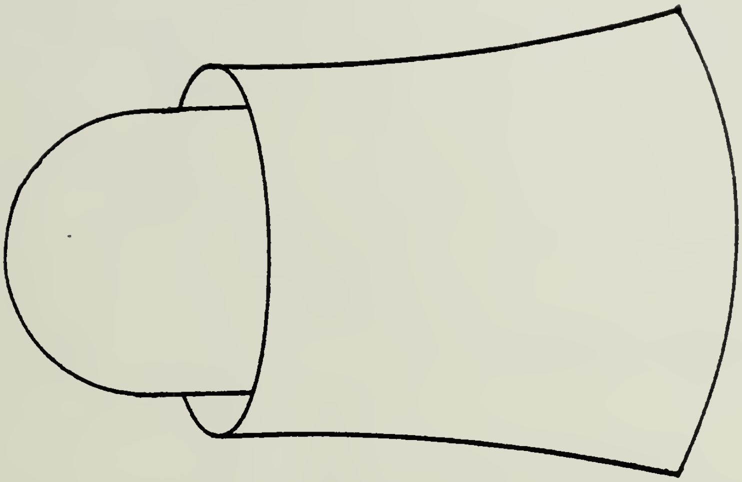

Figure II-1 Supersonic Inlet With Blunt Centerbody

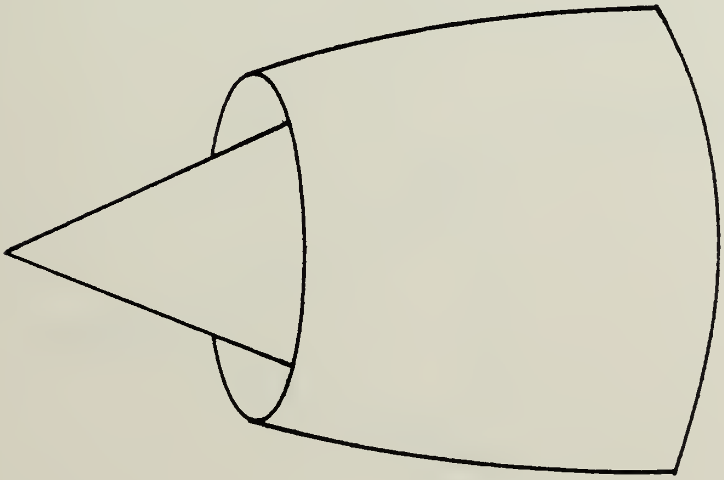

Figure II-2 Supersonic Inlet With Conical Spike

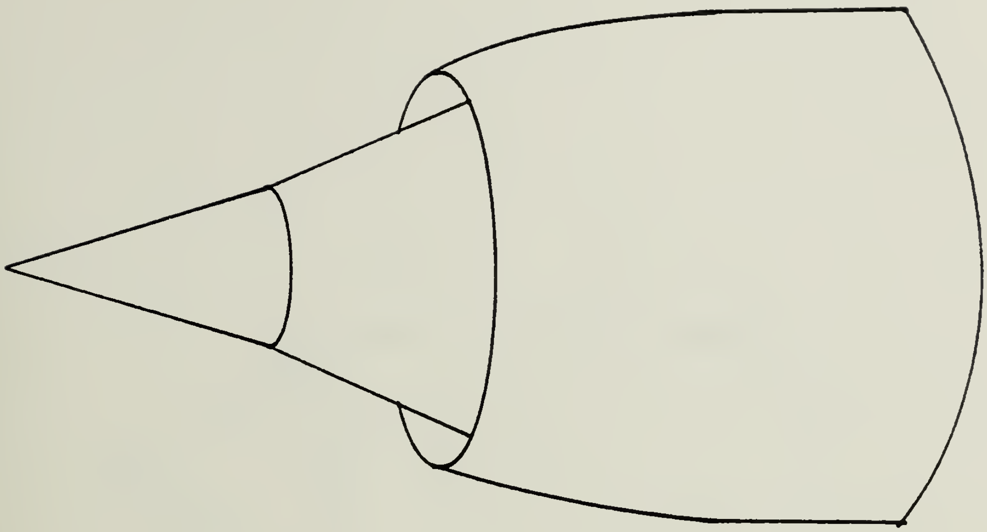

Figure II-3 Supersonic Inlet (variation)

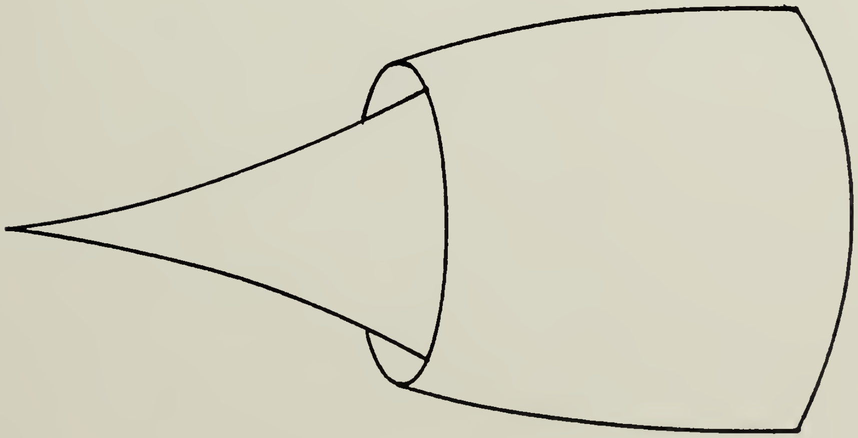

Figure II-4 Supersonic Inlet With Isentropic Spike

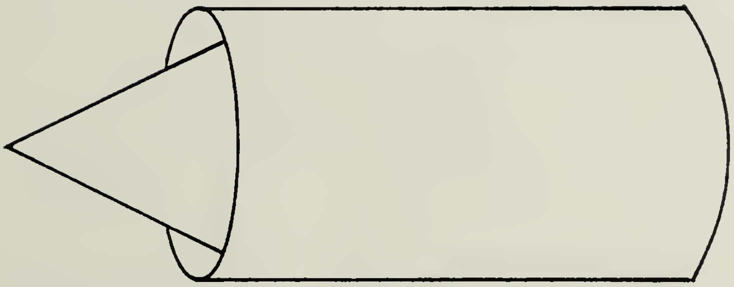

Figure II-5 Cylindrical Analog Of Busemann Biplane Inlet

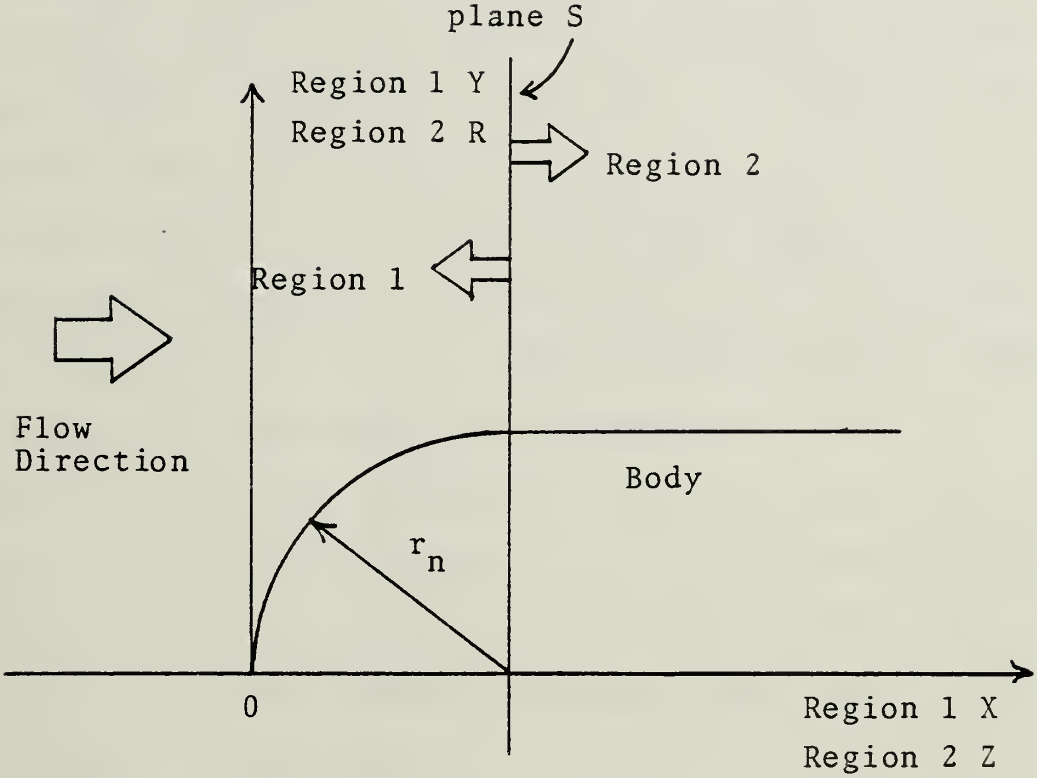

Figure II-6 Flow Regions Around A Blunt Nosed Body

in Figure II-6. The coordinates for region 1 are X and Y, which are the symbols used in the NASA Ames computer printout. The coordinates for region 2 are R and Z, also illustrated in Figure II-6. Each of the regions has different reference values and symbols for the flow properties. Appendix A lists the reference values and symbols.

In a real ramjet, the sizing of the inlet capture area, throat area and inlet area can dramatically vary the performance at different Mach numbers. The importance of the effect the inlet plays on performance is paramount.

Figure II-7 shows the magnitude of pressure losses as a fraction of total pressure recovery. As can be clearly seen, the majority of loss is due to boundary layer growth. However, as the flight Mach number increases, note that all the losses increase in magnitude.

For a conical inlet, the oblique shock losses can readily be calculated. The overall pressure recovery value of 0.72, for Mach 3.0 flow, can be obtained from Figure II-7.

For the blunt nosed body, $p_t/p_{t\infty}$ is tabulated in the NASA Ames printout. This corresponds to p_{t2}/p_{t1}, the oblique shock losses, in Figure II-8. To account for the varying pressure recovery values within the annulus, a mass weighted average will be used. This concept will be discussed in Section II-C-3.

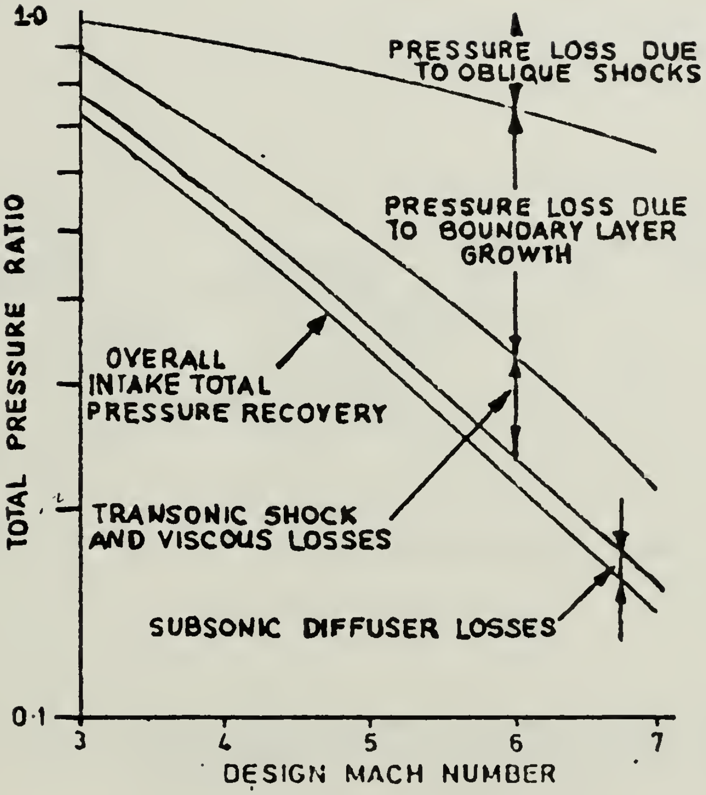

Figure II-7 Magnitude Of Pressure Losses (Reproduced from Ref. 4, p. 64)

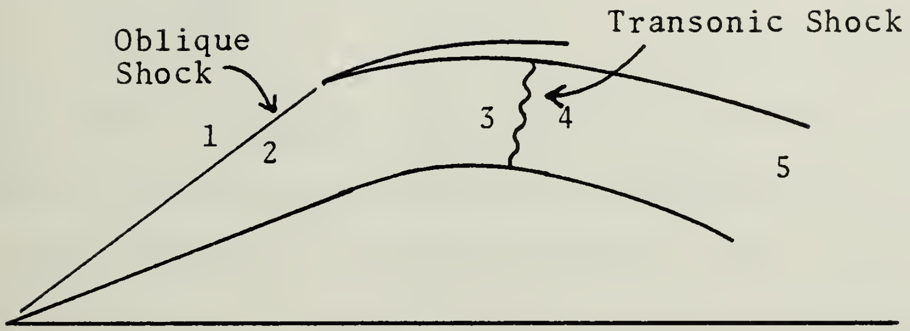

Figure II-8 Identification Of Locations For Description Of Pressure Recovery Losses In A Conical Inlet

Total pressure ratio, or pressure recovery, is defined as π_d. From Figure II-8,

$$\pi_d = \frac{p_{t5}}{p_{t1}} = \frac{p_{t2}}{p_{t1}} \frac{p_{t5}}{p_{t2}} \tag{1}$$

By defining π_d' as equal to p_{t2}/p_{t1}, the pressure recovery becomes

$$\pi_d = \pi_d' \frac{p_{t5}}{p_{t2}} \tag{2}$$

The value of p_{t5}/p_{t2} can be determined from Figure II-7. The value of p_{t5}/p_{t2} represents the accumulation of losses in an inlet due to the subsonic diffuser loss, p_{t5}/p_{t4}; transonic shock and viscous losses, p_{t4}/p_{t3}; and pressure loss due to boundary layer growth, p_{t3}/p_{t2}. The value of p_{t5}/p_{t2} is obtained from Figure II-7 as a ratio of overall inlet pressure recovery to oblique shock losses. For Mach 3.0 flow

$$\frac{p_{t5}}{p_{t2}} = \frac{0.72}{0.97} = 0.7423$$

The value of π_d' was calculated using the flow field calculations in the NASA Ames printout. The overall effect of the reduced recovery ratio is that the engine efficiency and the pressure ratio at the nozzle exit is changed. In turn, the

change in the pressure ratio may cause over or under expanded flow from the exit nozzle [Ref. 3].

C. FLOW FIELD DESCRIPTION IN THE VICINITY OF A BLUNT NOSE

For the blunt nosed centerbody at zero angle of attack, the flow field is axisymmetric with respect to the centerline of the projectile. The calculation of pressure recovery and ramjet performance is greatly simplified.

1. Determination Of Capture Streamline

Inherent to the analysis of ramjet performance is the determination of the mass flow rate of air at the annulus of the inlet, $\dot{m}_L$. After determining the mass flow rate, $\dot{m}_L$, the streamline coordinates will be determined at various points by equating the local mass flow to the mass flow at the lip. From these coordinates, the additive drag and coefficient of additive drag for the projectile at a particular Mach number will be determined. Two approaches for calculating the streamtube points were tried and will be discussed here.

a. Mass Flow Method

The first method involves mass flow analysis. The mass flow through any cross section of the particular streamtube will equal that of the mass flow through the annulus. Of particular interest is the radius of the capture area, r_s, on the bow shock wave. The air captured by this area goes into the inlet. The remainder of the air spills

past the inlet and affects the performance of the projectile by adding to the total vehicle drag with a term called additive drag, D_a.

The mass flow at the lip is given as

$$\dot{m}_L = \int_{body}^{lip} \rho_L \; u_L \; dA \qquad (3)$$

Where ρ_L is the density, dA the elemental area and u_L the velocity component normal to that area. From the continuity equation, the mass flow at the shock front is

$$\dot{m}_s = \rho_s \pi r_s^2 \; u_s \qquad (4)$$

Refer to Figure II-9. By equating equations 3 and 4

$$\rho_s \pi r_s^2 \; u_s = \int_{body}^{lip} \rho_L \; u_L \; 2\pi r_L \; dr_L \qquad (5)$$

By normalizing the distances involved to the nose radius and by dividing by ρ_∞ and v_m, to allow use of the NASA Ames printout values in region 2 , the equations become

$$\frac{r_s^2 \; u_s}{r_n^2 \; v_m} = 2 \; \frac{\rho_{t\infty}}{\rho_\infty} \int_{body}^{lip} \rho_2' \; u_2' \; r' \; dr' \qquad (6)$$

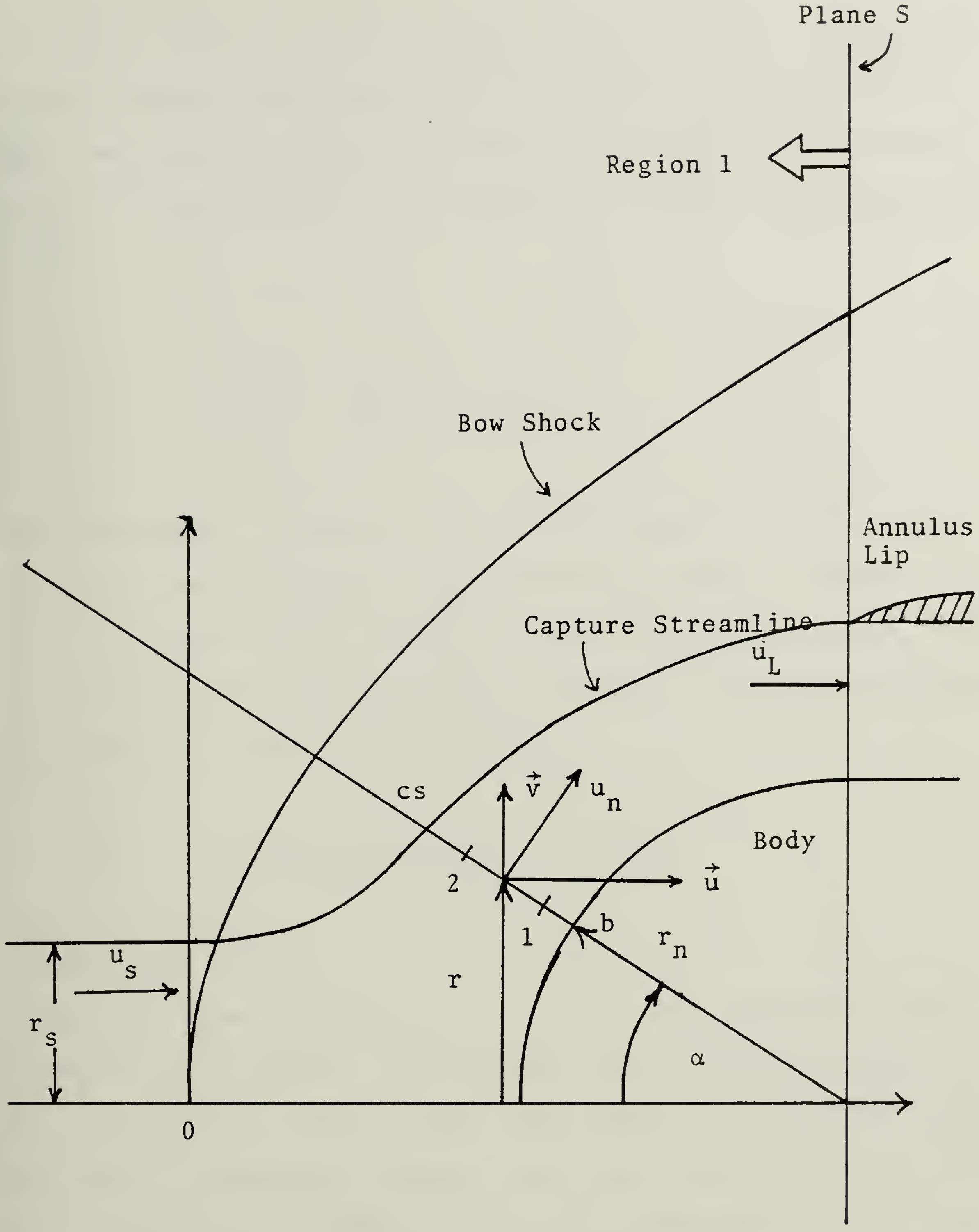

Figure II-9 Flow Geometry Around The Blunt Nose Showing Bow Shock, Streamtube And Body Locations

where $u_2' = u_L/v_m$; $\rho_2' = \rho_L/\rho_{t\infty}$; and $r' = r/r_n$. The primed values are the tabulated values from the NASA Ames printout and the subscript refers to the applicable flow region defined in Figure II-6. Q_∞ is defined as u_s/v_m, and equation 6 becomes

$$\frac{r_s^2}{r_n^2} = \frac{2\ \rho_{t\infty}}{Q_\infty\ \rho_\infty} \int_{\text{body}}^{\text{lip}} \rho_2'\ u_2'\ r'\ dr' \tag{7}$$

The integrand in equation 7 was plotted and the area under the curve calculated for the desired lip radius. Since $r_n = 1.0$ inches, $Q_\infty = 0.80174$, $\rho_\infty/\rho_{t\infty} = 0.07623$ at Mach 3 and the integral from body to lip is 0.00805, r_s can be determined. For Mach 3 airflow, with $r_L = 1.2$

$$r_s^2 = \frac{2}{(0.80174)(0.07623)}\ (0.00805)$$

Hence, $r_s = 0.5133$.

Table II-1 shows r_s for Mach 3.0 and a nose centerbody radii equal to 1.00 inches. The maximum value of the lip radius is 1.854 inches. This is the size imposed by the constraints of the 5"/54 handling system. Now the streamline locations at different flow field points can be calculated. The computer program used is described in Appendix B. The flow geometry is shown in Figure II-9.

Table II-1

Capture Radius, r_s, As A Function Of Lip Radius, r_L, For r_n Equal To 1.0 Inch At Station Z=1.00

r_L (inches)	r_s (inches)
1.1000	0.3821
1.2000	0.5883
1.3000	0.7765
1.4000	0.9610
1.5000	1.1474
1.6000	1.3353
1.7000	1.5231
1.8000	1.7066
1.8540	1.8086

The mass flow rate across a line of constant angle, α, is given by the following equation

$$\dot{m}_\alpha = \int_b^{cs} \rho \, u_n \, dS \tag{8}$$

where b refers to the body and cs refers to the capture streamline in Figure II-9. From Figure II-10, an element of area on the line of constant α is given as

$$dS = 2\pi r dl \tag{9}$$

and dl can be related to the angle α by

$$dl = \frac{dr}{\sin\alpha} \tag{10}$$

Hence, dS in terms of dr becomes

$$dS = 2\pi r \frac{dr}{\sin\alpha} \tag{11}$$

From Figure II-11, an angle β is defined so that

$$\beta = \tan^{-1}(v/u) \tag{12}$$

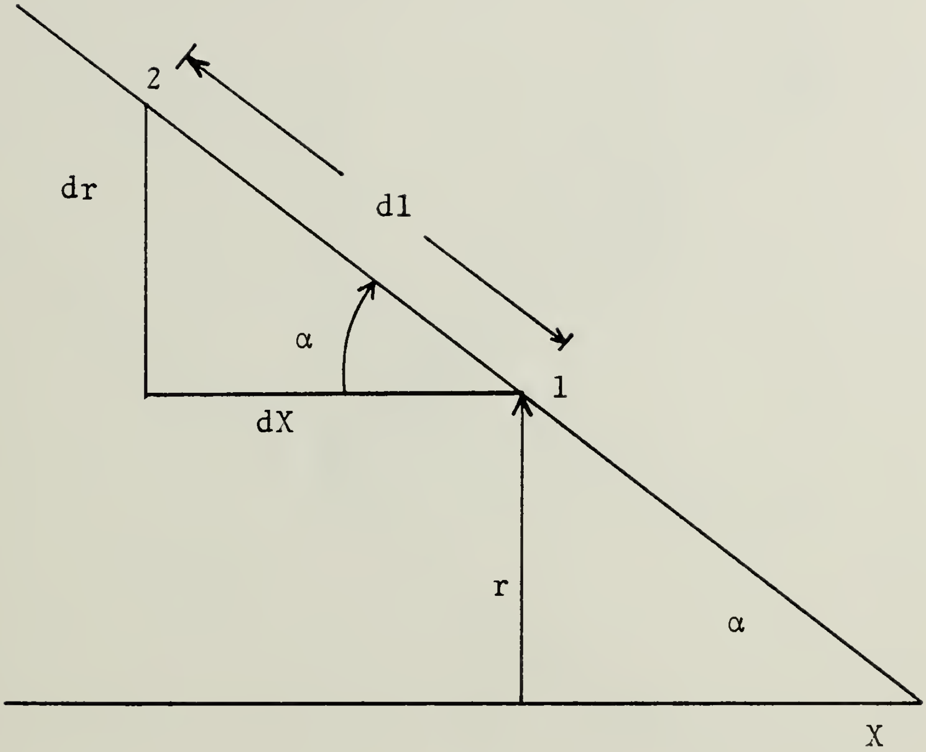

Figure II-10 Magnified View Of Geometry Between Points 1 And 2 Of Figure II-9

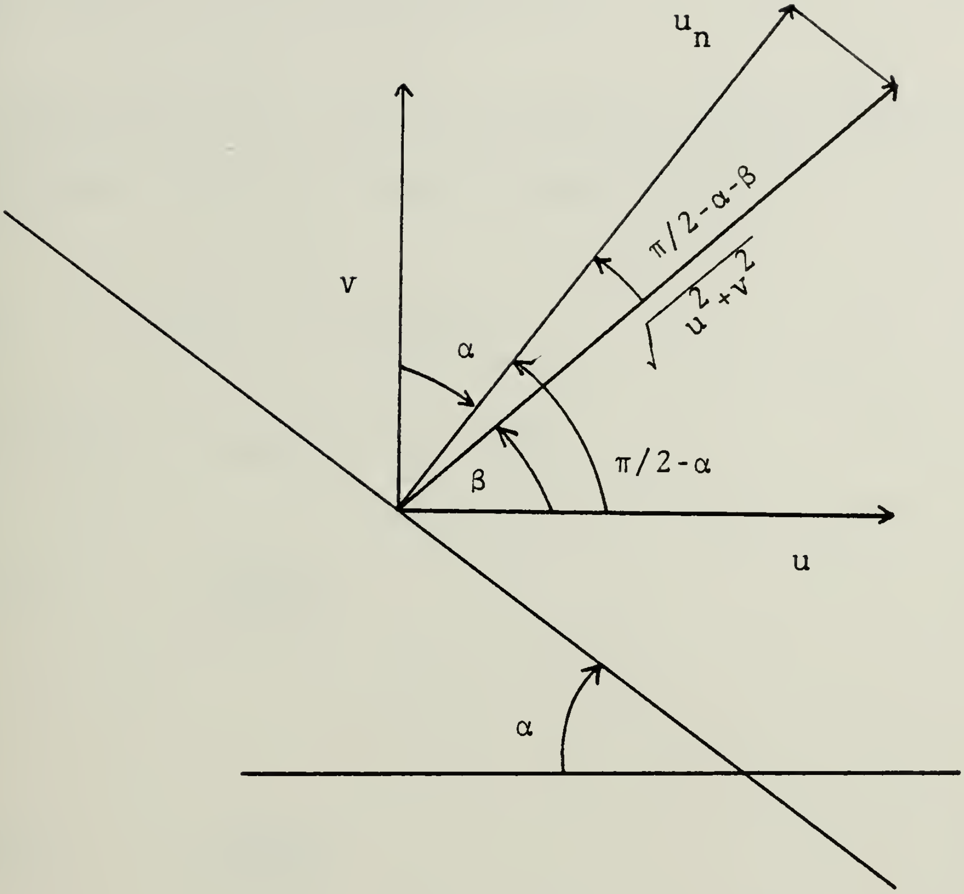

Figure II-11 Geometry To Determine Component Of Velocity Normal To The Area For Integration Of Mass Flux

Hence, the normal component of the velocity becomes

$$u_n = \sqrt{u^2 + v^2}\ \cos(\pi/2 - \alpha - \beta) \tag{13}$$

With the substitution of a trigonometric identity for the cosine term, equation 13 can be simplified to

$$u_n = \sqrt{u^2 + v^2}\ \sin(\alpha + \beta) \tag{14}$$

The geometry of Figure II-11 gives

$$\cos\beta = \frac{u}{\sqrt{u^2+v^2}} \tag{15}$$

and

$$\sin\beta = \frac{v}{\sqrt{u^2+v^2}} \tag{16}$$

Using equations 15 and 16 and substituting into equation 14 leaves

$$u_n = \sqrt{u^2+v^2}\ \left(\frac{u \sin\alpha}{\sqrt{u^2+v^2}} + \frac{v \cos\alpha}{\sqrt{u^2+v^2}}\right) \tag{17}$$

The value of airflow normal to the cross sectional area dS then becomes

$$u_n = u \sin\alpha + v \cos\alpha \qquad (18)$$

Substituting equations 11 and 18 into equation 8, the following equation is obtained

$$\dot{m}_\alpha = \int_b^{cs} (\rho 2\pi r)(u \sin\alpha + v \cos\alpha)/(\sin\alpha)\, dr \qquad (19)$$

This becomes, after manipulation

$$\dot{m}_\alpha = \int_b^{cs} \rho\ 2\pi r\ (u + v\ \cot\alpha) dr \qquad (20)$$

The mass flow given by the above equation through the streamtube at the radial line of constant angle α must equal the mass flow through the nose capture area. Multiplying the integrand by $(r_n/r_n)^2$ and dividing both sides by the mass flow at the bow shock, equation 4, gives the following result

$$1 = \int_b^{cs} 2 \left(\frac{r_n}{r_s}\right)^2 \frac{\rho}{\rho_s} \frac{r}{r_n} \left[\frac{u}{u_s} + \frac{v}{u_s}\right] \frac{dr}{r_n} \qquad (21)$$

In front of the projectile shoulder, equation 21 becomes

$$\left(\frac{r_s}{r_n}\right)^2 = 2 \int_b^{cs} \rho_1' \, r' \, (u_1' + v_1' \cot\alpha) dr' \qquad (22)$$

For region 2 , which is after the shoulder, due to the different reference values equation 20 becomes

$$\left(\frac{r_s}{r_n}\right)^2 = \frac{2\rho_{t\infty}}{Q_\infty \rho_\infty} \int_b^{cs} \rho_2' \, r' \, (u_2' + v_2' \cot\alpha) dr' \qquad (23)$$

where in equations 22 and 23, the primed values are taken from the NASA Ames printout. In region 2 , α equals 90° and cotangent of α is zero.

b. Angular Method

The second method of streamtube calculation is by the angular method. A linear variation of the known flow field properties over small distances is assumed. The method starts at the lip and progressively moves forward along the body determining streamtube position.

Initially, the local velocity vector at the various flow field points must be plotted in polar notation. By averaging the velocity flow angles at two adjacent stations, an average angular value can be determined. As an example, for a lip radius of 1.2

$$\theta_{34} = (\theta_3 + \theta_4)/2 \qquad (24)$$

where θ_3 = local flow field velocity angle at station 3

θ_4 = local flow field velocity angle at station 4

θ_{34}= average angle between station 3 and 4 stream tube locations

θ_4, the flow field angle at the lip, is determined from linear interpolation of the known flow field angles. By varying θ_{43}, with θ_4 known, the value of θ_3 is determined. As a function of θ_{43}.

$$\theta_4 = 2\theta_{43} - \theta_3 \qquad (25)$$

θ_{43} is then plotted as a function of the radius of the streamtube, R_3 in this case.

By studying Figure II-12, the geometry of the field also determined θ_{43}.

$$\tan \theta_{43} = \left[\frac{R_4 - R_3}{Z_4 - Z_3} \right] \qquad (26)$$

In the above equation, all quantities with the exception of R_3 are known. θ_{43} is then plotted versus R_3.

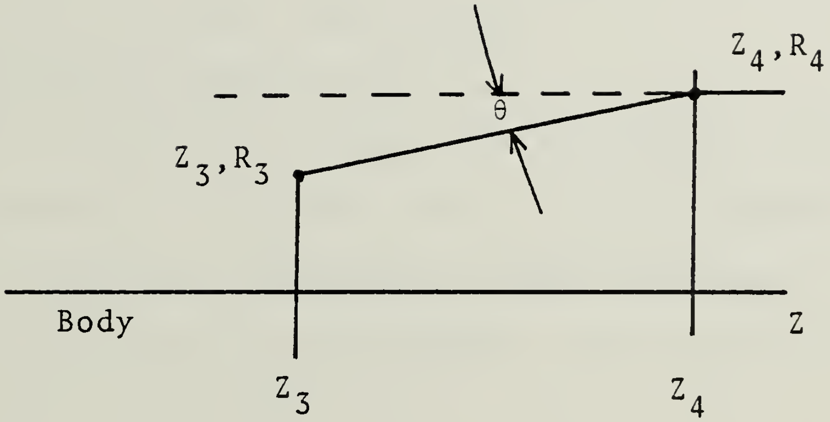

Figure II-12 Flow Field Geometry For The Angular Method Of Streamtube Determination

The intersection of these two curves determines R_3 and θ_{43}, and hence θ_3 can be determined by interpolation. In this manner, the streamtube points are calculated for the desired lip radius. This method produces comparable results to the mass flow analysis but is not accurate enough proceeding past the nose of the projectile. Additionally, the process is extremely slow and complicated.

2. Determination Of Additive Drag

The additive drag is calculated by a computer program discussed in Appendix C. Assuming that the points defining the edge of the streamtube determined by mass flow analysis can be connected by straight line segments, the equation for additive drag can be written as

$$D_a = \Sigma(p_i - p_\infty)A_i \sin\theta_i \qquad (27)$$

where p_i equals the average pressure at the data points i and i+1; θ_i is the angle of the straight line segment between the points i and i+1 measured from the projectile axis; and A_i is the surface area of the cone between the i and i+1 data points. The geometry is shown in Figure II-13.

The coefficient of additive drag (C_{dad}) can be determined by dividing equation 27 by q_∞ and reference area, A_r,

$$C_{dad} = \frac{2\ \Sigma\ p_\infty(\frac{p_i}{p_\infty} - 1)\ A_i \sin\theta_i}{\gamma p_\infty\ M_\infty^2\ A_r} \qquad (28)$$

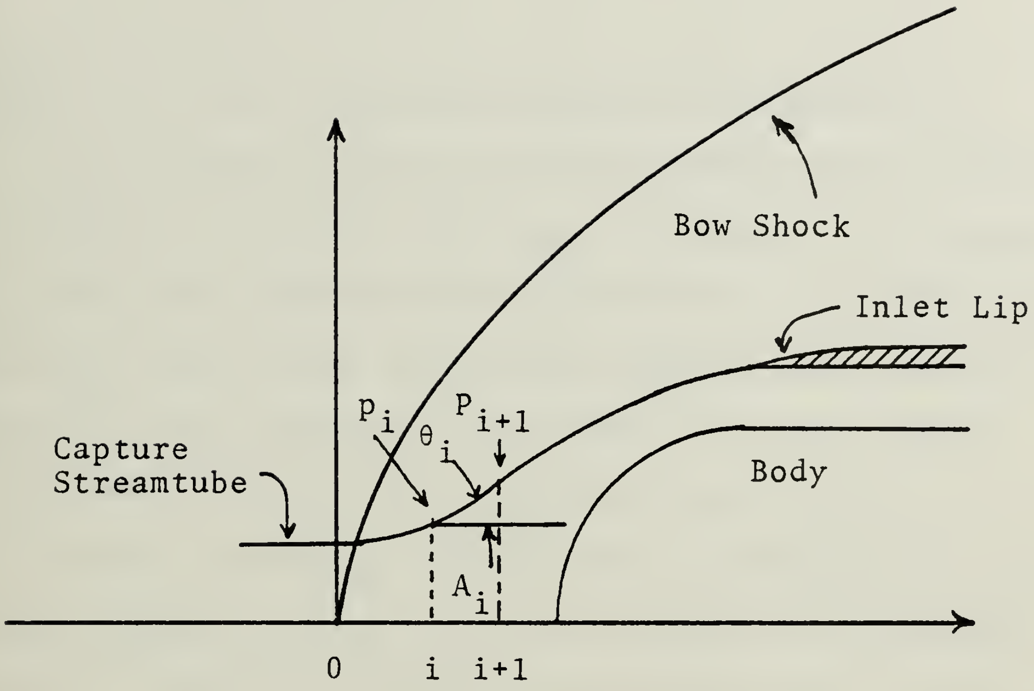

Figure II-13 Geometry For Additive Drag Calculation

The reference area, A_r, is taken to be the base of the five inch projectile. Simplification of equation (28) leads to

$$C_{dad} = \frac{2}{\gamma M_\infty^2} \Sigma \left(\frac{p_i}{p_\infty} - 1\right) \frac{A_i}{A_r} \sin\theta_i \qquad (29)$$

Equation (29) is the equation programmed in Appendix C.

The program utilizes the points generated by the program in Appendix B to calculate C_{dad}. However, it is important to scale the nose capture radius from a centerbody radius of one inch to the actual centerbody radius on the projectile. Previously r_L was fixed at 1.854 inches. A ratio between the centerbody and lip radii is defined as $x = r_L/r_n$.

The lip radius, r_L, is fixed by the dimensions of the handling equipment, and r_n can be determined as a function of the ratio x. Table II-2 displays the values of x, r_n, C_{dad}, and mass flow ratio. Mass flow ratio is defined as $\dot{m}_s/\dot{m}_s^o$. The symbols $\dot{m}_s$ and $\dot{m}_s^o$ are defined in Table II-2.

3. Average Stagnation Pressure Ratio At The Inlet Lip

The stagnation pressure at the annulus of the inlet is a function of radius. A mass weighted average stagnation pressure was calculated. The average pressure recovery will be multiplied by a factor of p_{t5}/p_{t2} to obtain total pressure recovery as discussed in section II.

Table II-2

Summary Of Radius Of Capture Streamtube, Additive Drag Coefficient, And Mass Flow Ratio

		For r_L = 1.854 in.			
$x = r_L/r_n$	r_s/r_n	r_n	r_s	C_{dad}	$\dot{m}_s/\dot{m}_s^o$
1.1	0.3821	1.6855	0.6440	0.3726	0.121
1.2	0.5883	1.5450	0.9089	0.2956	0.240
1.3	0.7765	1.4262	1.1074	0.2299	0.357
1.4	0.9610	1.3243	1.2727	0.1775	0.471
1.5	1.1474	1.2360	1.4181	0.1319	0.595
1.6	1.3353	1.1588	1.5473	0.0928	0.697
1.7	1.5231	1.0906	1.6611	0.0588	0.803
1.8	1.7066	1.0300	1.7578	0.0304	0.899
1.854	1.8086	1.0000	1.8086	0.0179	0.952

$\dot{m}_s$ is defined by equation (4); $\dot{m}_s^o$ is obtained from equation (4) with r_s replaced by r_L

The mass weighted average of pressure recovery is given by

$$\pi_d' = \frac{\bar{p}_t}{p_{t\infty}} = \sum_{j=1}^{x} \left(\frac{p_t}{p_{t\infty}}\right)_j \frac{\dot{m}_j}{\dot{m}_L} \qquad (30)$$

where the subscript j refers to the jth streamtube within the inlet, $\dot{m}_j$ is the mass flow of the jth streamtube and $\dot{m}_L$ is the total mass flow through the entire inlet as defined by equation 3. This geometry is further shown in Figure II-14. If the inlet lip splits a streamtube the values for pressure recovery and mass flow are linearily interpolated to achieve the average pressure recovery. The values of $(p_t/p_{t\infty})_j$ were taken from the NASA Ames printout.

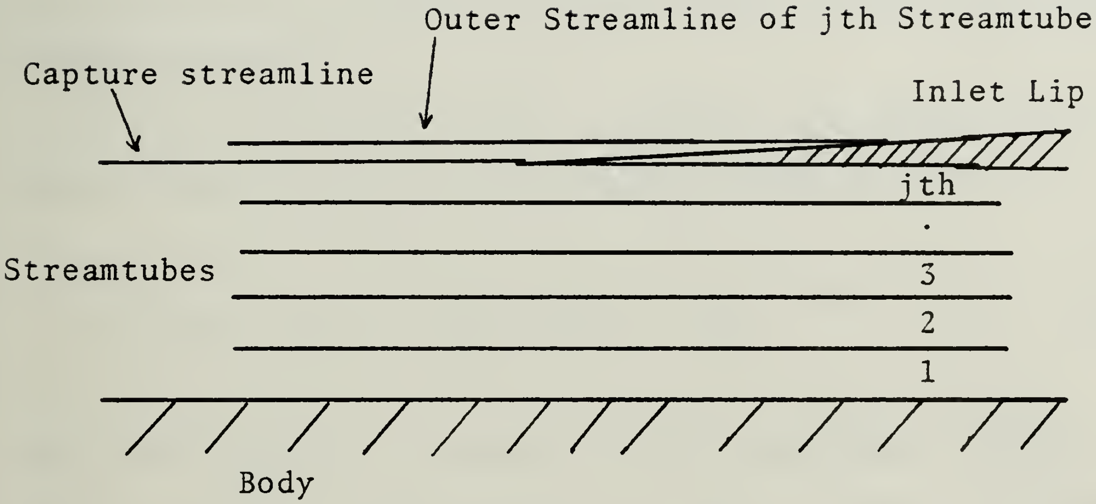

Figure II-14 Geometry Of Streamtubes At The Inlet Annulus Used To Calculate Average Stagnation Pressure, π_d'

III. CALCULATION OF RAMJET PERFORMANCE

A. PERFORMANCE EQUATIONS

Ramjet engine performance can be quantified by the specific thrust, specific fuel consumption, and the coefficient of thrust. Performance equations will be developed for each of the above performance criterion which include the concept of additive drag.

If one dimensional flow is assumed, the thrust, F, of a ramjet engine is described by Netzer [Ref. 5] as

$$F = \dot{m}_e v_e - \dot{m}_o v_o - D_a + A_e(p_e - p_o) \qquad (31)$$

where the subscript e refers to exit conditions and the subscript o refers to the inlet conditions. Term 1 is defined as jet or gross thrust, term 2 is the ram drag, term 3 is the additive drag and term 4 is the pressure thrust. If ideal expansion is assumed ($p_e = p_o$), equation 1 becomes

$$F = \dot{m}_e v_e - \dot{m}_o v_o - D_a \qquad (32)$$

Now, defining the fuel air ratio, f, as

$$f = \dot{m}_f/\dot{m}_o \qquad (33)$$

the mass flow through the ramjet exit can be written as

$$\dot{m}_e = \dot{m}_o + \dot{m}_f = \dot{m}_o \ (1 + f) \qquad (34)$$

The fuel air ratio, f, is generally much less than one. Combining equations 32 and 34 allows the total thrust to be written as

$$F = \dot{m}_o(v_e - v_o) - D_a \qquad (35)$$

Factoring v_o from the first term on the right hand side gives

$$F = \dot{m}_o v_o \ (\frac{v_e}{v_o} - 1) - D_a \qquad (36)$$

Combining equation 36 with the definition of Mach number and the speed of sound, a_o, inserting an expression for combustor energy balance and assuming that the stagnation pressure through the inlet, burner and nozzle are taken as to be constant allows thrust to be written as a function of fuel air ratio, heating value of the fuel and the combustion temperature.

$$F = \dot{m}_o v_o \ [\sqrt{1 + \frac{hf}{C_p T_{to}}} -1] - D_a \qquad (37)$$

The specific thrust is obtained from equation (37) by dividing by the mass flow rate, $\dot{m}_o$. Units of $\dot{m}_o$ are slug/sec and specific thrust is usually in units of $lb_f/(lb_m/sec)$.

$$SF = \frac{F}{\dot{m}_o g} \tag{38}$$

The specific fuel consumption, SFC, is defined as the unit mass flow of fuel per hour per pound thrust. Expressed in the form of an equation.

$$SFC = \frac{3600 \dot{m}_f g}{F} \tag{39}$$

In equation (39) $\dot{m}_f$ has units of slug/sec. Inserting equation 37 yields

$$SFC = \frac{3600 \dot{m}_f \, g}{\dot{m}_o v_o \left[\sqrt{1 + \frac{hf}{C_p T_{to}}} - 1\right] - D_a} \tag{40}$$

where $\dot{m}_f$ = mass fuel flow rate (slugs/sec)
g = gravitational constant
h = heating value of fuel (BTU/lb)
f = fuel air ratio
C_p = specific heat capacity (BTU/lb °R)
T_{to} = inlet stagnation temperature

The thrust coefficient is defined as

$$C_f = \frac{F}{q_o A_r} \tag{41}$$

where q_o is the dynamic pressure and A_r is the reference area. The reference area is the base area of the five inch projectile. For a ramjet, mass flow at the inlet is given as

$$\dot{m}_o = A_o v_o \rho_o \tag{42}$$

Combining equations (37), (41) and (42) gives

$$C_f = \frac{2A_o}{A_r} \left[\sqrt{1 + \frac{hf}{C_p T_{to}}} - 1 \right] - \frac{D_a}{q_o A_r} \tag{43}$$

The preceding equations were derived for a ramjet engine without internal losses. Losses in a ramjet engine that should be accounted for are

a) loss of stagnation pressure in the diffuser, π_d
b) loss of stagnation pressure in the burner, π_b
c) loss of stagnation pressure in the nozzle, π_n
d) combustion efficiency, η_b

These terms result in the generation of a common term, S_r, which does affect the calculation of ramjet performance. S_r is defined as

$$S_r = \left\{ \left[\frac{\left(\frac{1}{\pi_b \pi_d \pi_n}\right)^{\frac{\gamma-1}{\gamma}} - 1}{\frac{\gamma-1}{2} M_o^2} \right] \left[1 + \frac{\eta_b f h}{C_p T_{to}} \right] \right\}^{1/2} \tag{44}$$

The square root appearing in equations (38), (40) and (43) is replaced by S_r to give ramjet performance with internal losses and with an additive drag term. The performance equations becomes

$$SF = [\dot{m}_o M_o a_o (S_r - 1) - D_a]/\dot{m}_o g \tag{45}$$

$$SFC = \frac{3600 \dot{m}_f g}{F} \tag{46}$$

$$C_f = \frac{2A_o}{A_r} (S_r - 1) - \frac{D_a}{q_o A_r} \tag{47}$$

The computer program developed by Fuhs [Ref. 6] was modified to compute the additive drag term. Holding the values of π_b, π_n and η_b constant, the performance of a ramjet engine with a blunt centerbody was predicted. The performance of a ramjet with a conical spike inlet as predicted by the program serves as a baseline measurement of performance.

IV. DISCUSSION OF RESULTS

A. PERFORMANCE CRITERION

Performance of a ramjet engine can be quantified in different ways. For purposes of this report, the performance was compared to a ramjet baseline configuration using a conical inlet spike; the inlet capture area is 0.0123 ft^2 [Ref. 7].

The performance of a ramjet with the blunt centerbody configuration was calculated for a range of fuel/air ratios. Performance is specified on the basis of combusiton exit temperature (T_{t3}), specific fuel consumption and excess thrust. Of special interest is performance when C_f equals C_D. The value of C_D, which was obtained from White [Ref. 8], was 0.349.

The combustor exit temperature is calculated by the ramjet performance program as an output variable. Current technology limits the steady combustor exit temperature to about 4400°R. The value chosen for analysis purposes is 4422°R. Above this temperature, the combustor and exit nozzle will melt, if run for a continuous period of time. The value of T_{t3} is generally less than T_{t3} at the stoichiometric fuel/air ratio for the hydrocarbon.

For the final seconds of flight, it is possible to boost the fuel/air ratio to the stoichiometric value. The boost

in fuel/air ratio will increase the amount of excess thrust available for terminal maneuvering. Since the GLM will explode at flight termination, the combustor exit temperature is of little importance in terminal flight.

A further basis for performance comparison is the effect on relative detection range of seeker aperture. Seeker aperture is equal to πr_n^2.

Specific fuel consumption (SFC) was chosen as a comparison standard because it provides a good measure of ramjet fuel efficiency. Excess thrust is used as a measure of the ability of the guided projectile to maneuver in the terminal phase of the encounter. Regardless of the seeker accuracy, lack of thrust above the amount of flight drag will result in the inability to pursue a maneuvering target. Excess thrust coefficient, C_{fe}, is calculated as

$$C_{fe}(T_{t3}) = C_f(T_{t3}) - C_D \qquad (48)$$

where C_D is airframe drag and $C_f(T_{t3})$ is the thrust coefficient for T_{t3}. Two values of T_{t3} are of interest. One is the maximum allowed combustor exit temperature for steady operation which is 4422°R. The other is T_{t3} for stoichiometric combustion which is 5968°R; stoichiometric fuel/air ratio is 0.06.

B. RESULTS OF CALCULATIONS

Figure IV-1 plots T_{t3} versus r_L/r_n at a value of $C_D = C_f$. As can be clearly seen, as the ratio of r_L/r_n increases, or as the centerbody shrinks, T_{t3} decreases. T_{t3} reaches the maximum sustained operating value of 4422°R when r_L/r_n is 1.63; r_L/r_n equal to 1.63 is the minimum value for sustained operation. For stoichiometric combustion (f=0.06), r_L/r_n could possibly be reduced to a value as small as 1.50.

From the minimum value of r_L/r_n obtained in Figure IV-1, Figure IV-2 is entered. Figure IV-2 is a plot of excess thrust coefficient versus r_L/r_n and of stoichiometric excess thrust coefficient versus r_L/r_n. Stoichiometric excess thrust is defined as C_f at stoichiometric conditions (f=0.060) minus C_D.

Using a value of r_L/r_n equal to 1.63, the ramjet will have excess maneuvering thrust only at values of r_L/r_n greater than 1.63. Use of stoichiometric fuel/air mixture, during the last seconds of the encounter with a maneuvering target, results in excess thrust being generated for r_L/r_n greater than 1.51.

Figure IV-3 is a graph of the specific fuel comsumption (SFC) versus r_L/r_n. SFC decreases as r_L/r_n increases. The baseline ramjet has a SFC equal to 2.02 for C_D equal to C_f. For r_L/r_n equal to 1.63, the ramjet with a blunt nose has 65% higher SFC.

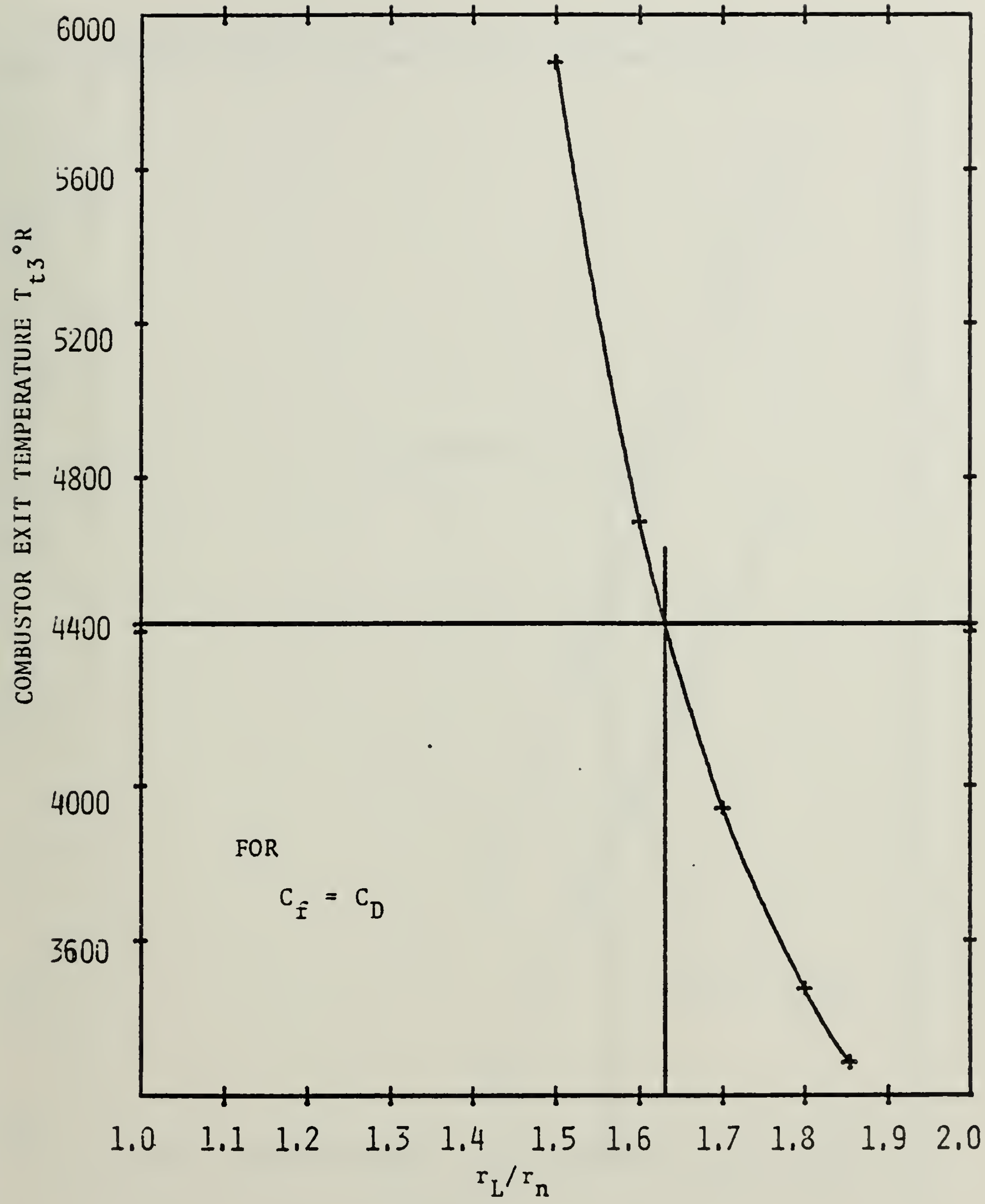

Figure IV-1 Combustor Exit Temperature As a Function Of r_L/r_n At $C_f = C_D = 0.349$

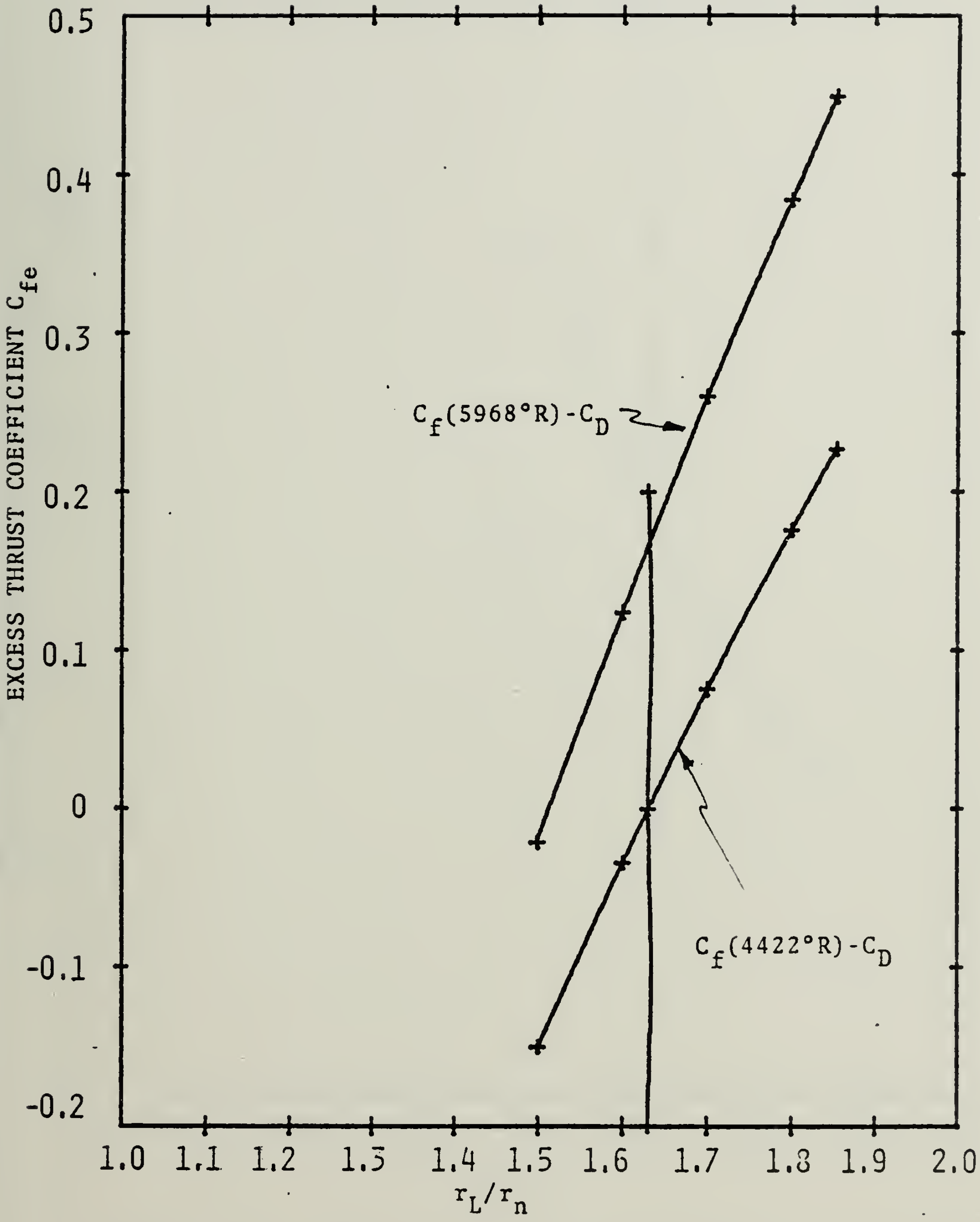

Figure IV-2 Excess Thrust Coefficient As A Function Of r_L/r_n

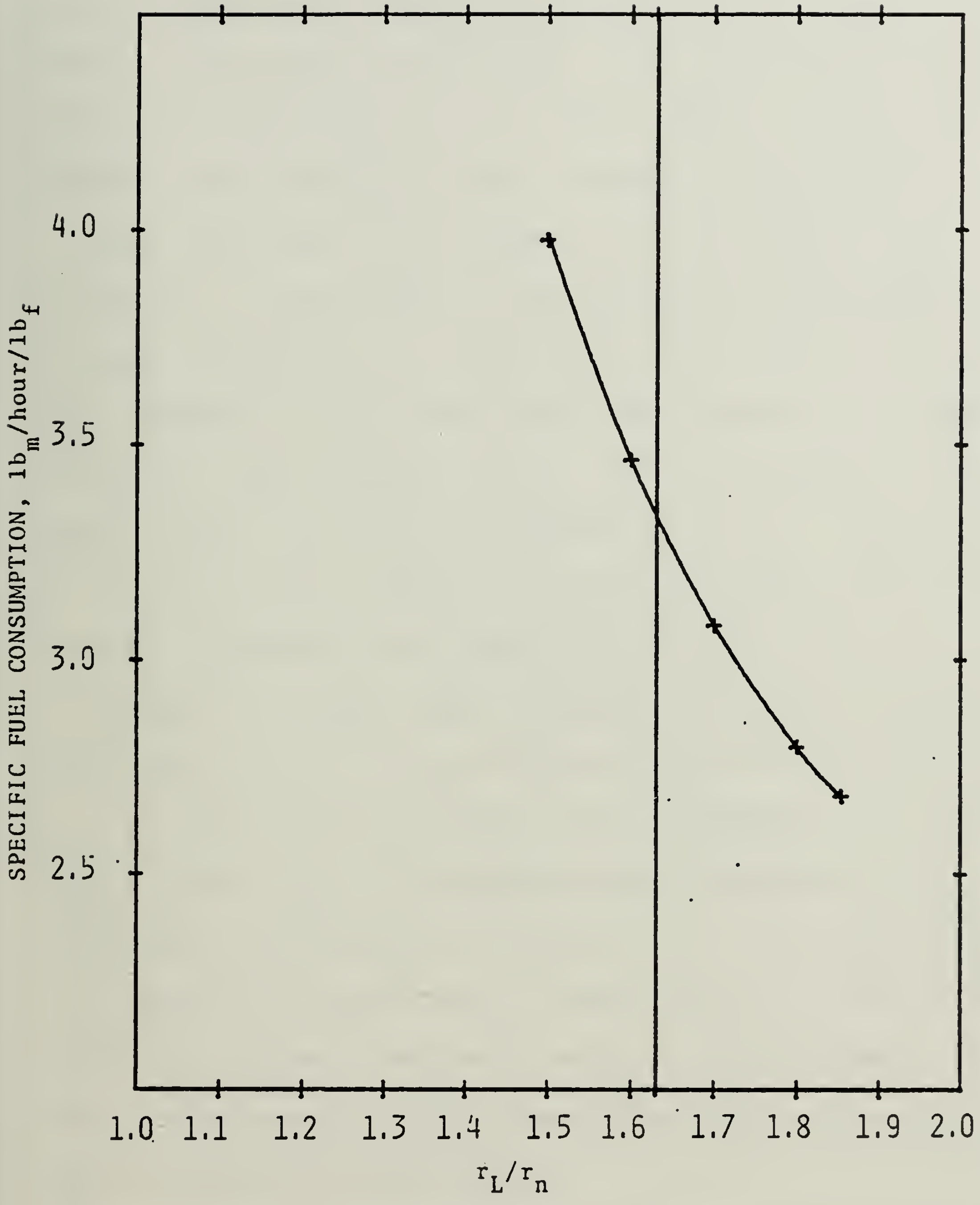

Figure IV-3 Specific Fuel Consumption As A Function Of r_L/r_n For Ramjet With Blunt Centerbody

Figure IV-4 is a plot of relative detection range of an IR seeker for various r_L/r_n. The signal-to-noise ratio of the IR seeker and, therefore, the detection range is proportional to the area of the lense. The lense area is directly related to the square of the lense radius. As r_L/r_n increases, the detection range decreases as $(r_n/r_L)^2$.

Mass flow ratio was defined in the text near Table II-3. The ratio is interpreted as the fraction of the mass flow actually captured, $\dot{m}_s$, relative to mass flow into an area πr_L^2. Figure IV-5 has mass flow ratio plotted as a function of r_L/r_n. Also Figure IV-5 has a plot of capture streamtube radius ratio, r_s/r_L, as a function of r_L/r_n. For the minimum value of r_L/r_n equal to 1.63, the capture radius ratio is 0.84. Likewise, the mass flow ratio is 0.70.

Figure IV-6 shows the variation of additive drag coefficient with r_L/r_n. At the minimum value of r_L/r_n of 1.63, C_{dad} is 0.085. The airframe drag coefficient is 0.349. Hence, C_{dad} is 24% of C_D. To understand the behavior of C_{dad} as a function of r_L/r_n refer to Figure IV-7. For r_L/r_n equal to 1.1, which is illustrated in Figure IV-7(a), the capture streamline between bow shock and lip of the annulus is steep. Also, the pressure is large near the axis. Consequently, C_{dad} is large for small r_L/r_n.

The greater the ratio of r_L/r_n becomes the better ramjet performance becomes. However, to achieve even marginal performance at $r_L/r_n = 1.63$, an unrealistic penalty in the

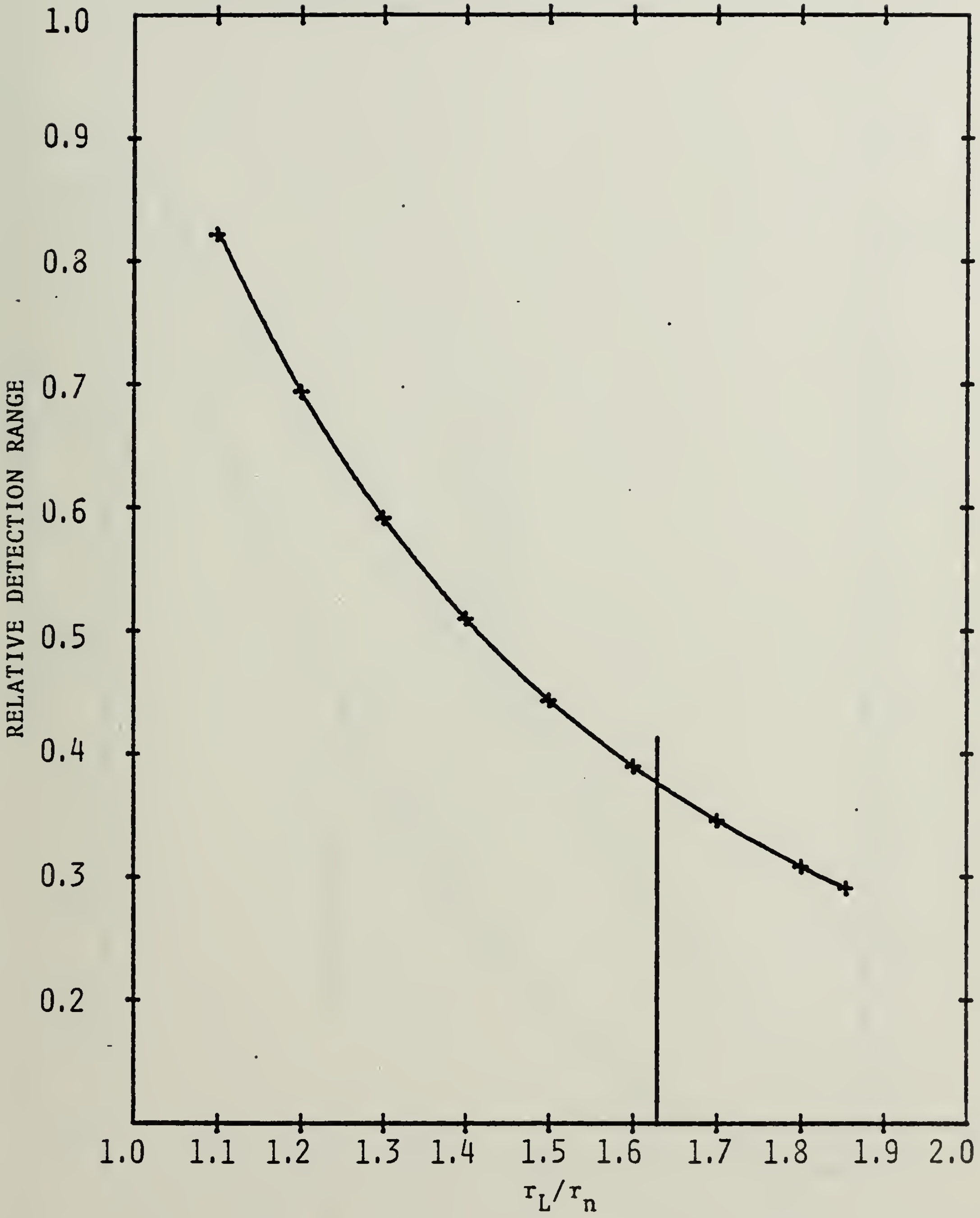

Figure IV-4 Relative Detection Range As A Function Of r_L/r_n

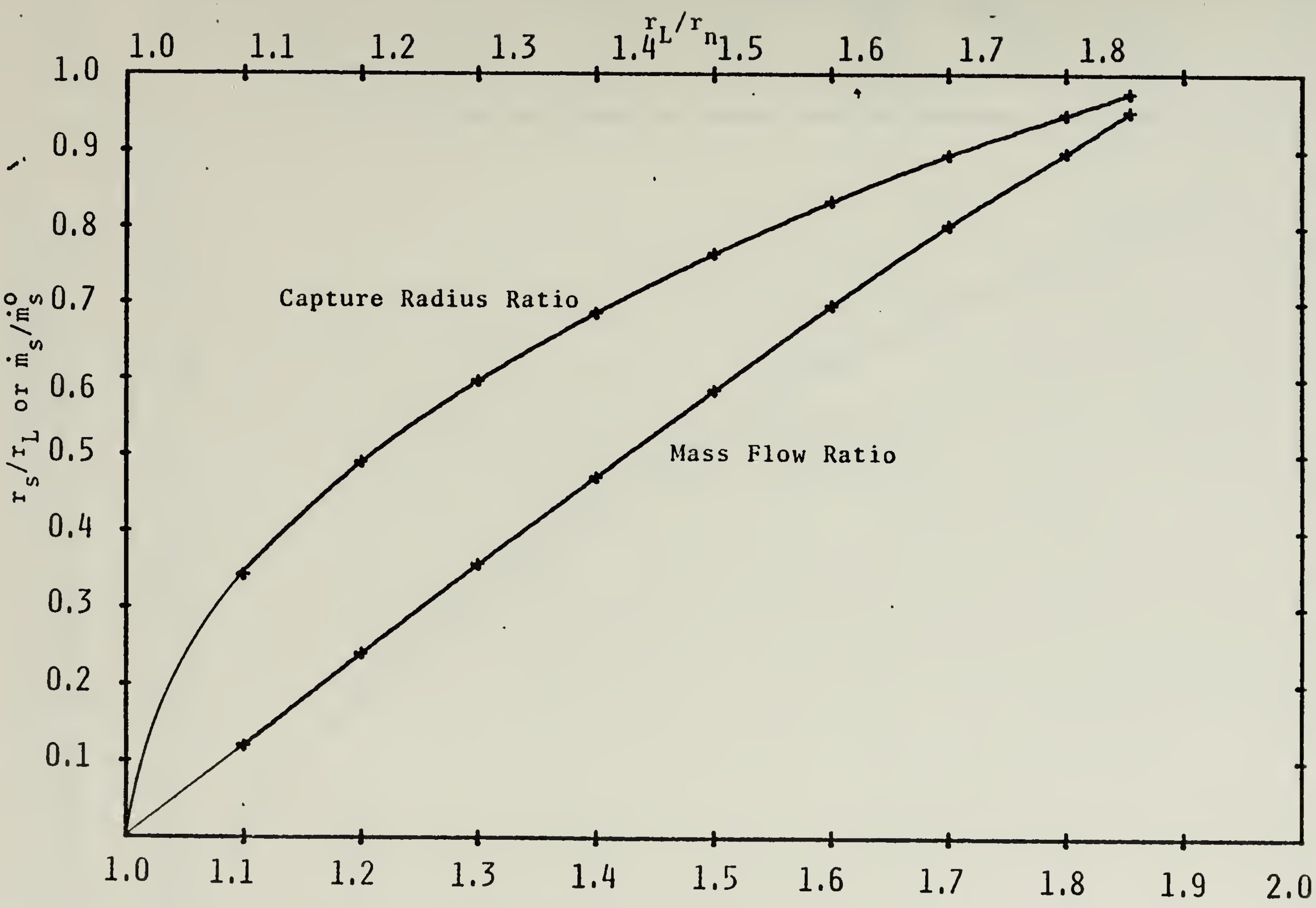

Figure IV-5 Mass Flow Ratio And Capture Radius Ratio As A Function Of r_L/r_n

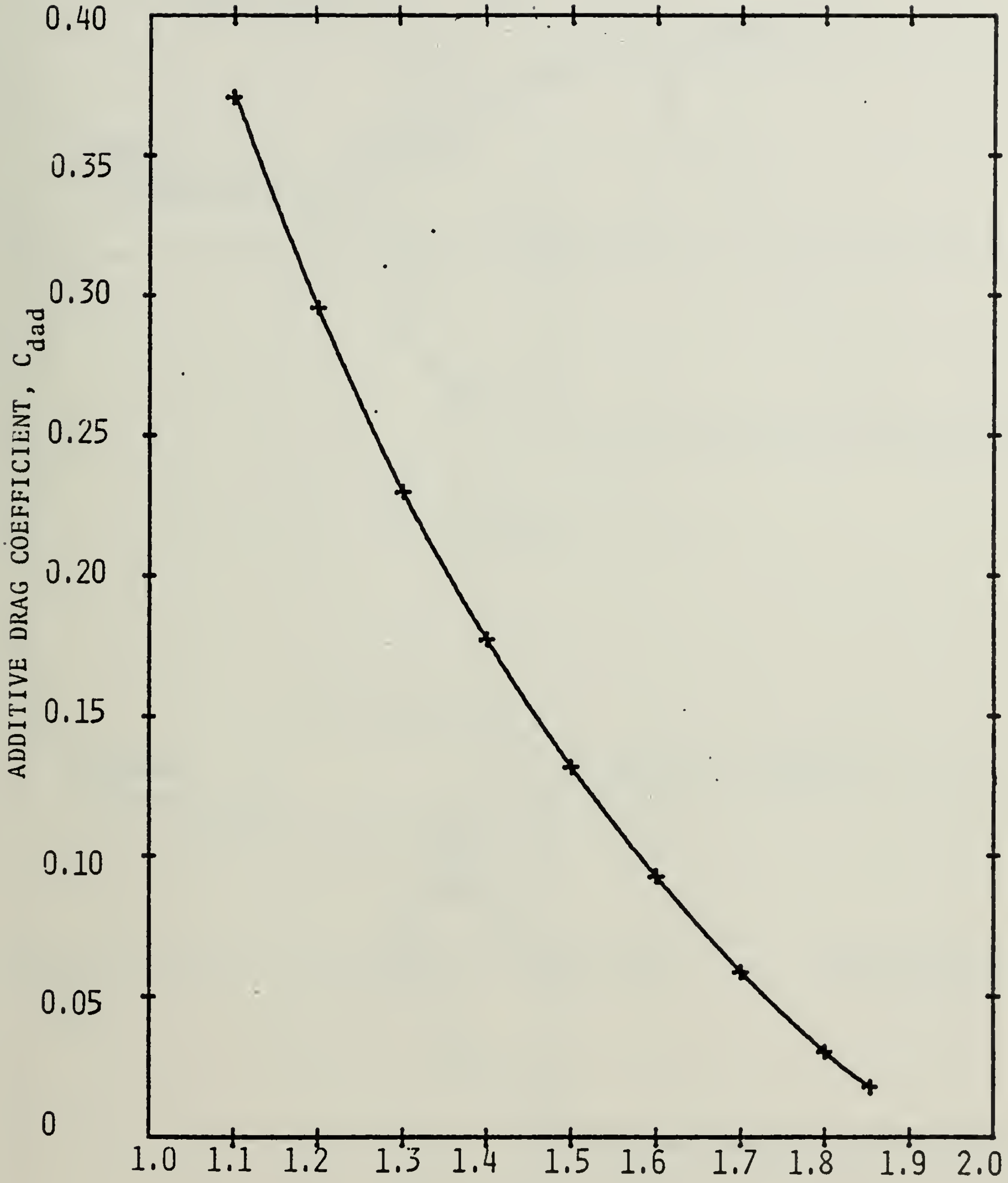

Figure IV-6 Additive Drag Coefficient As A Function Of r_L/r_n For An Inlet At The Shoulder (Z=1.00)

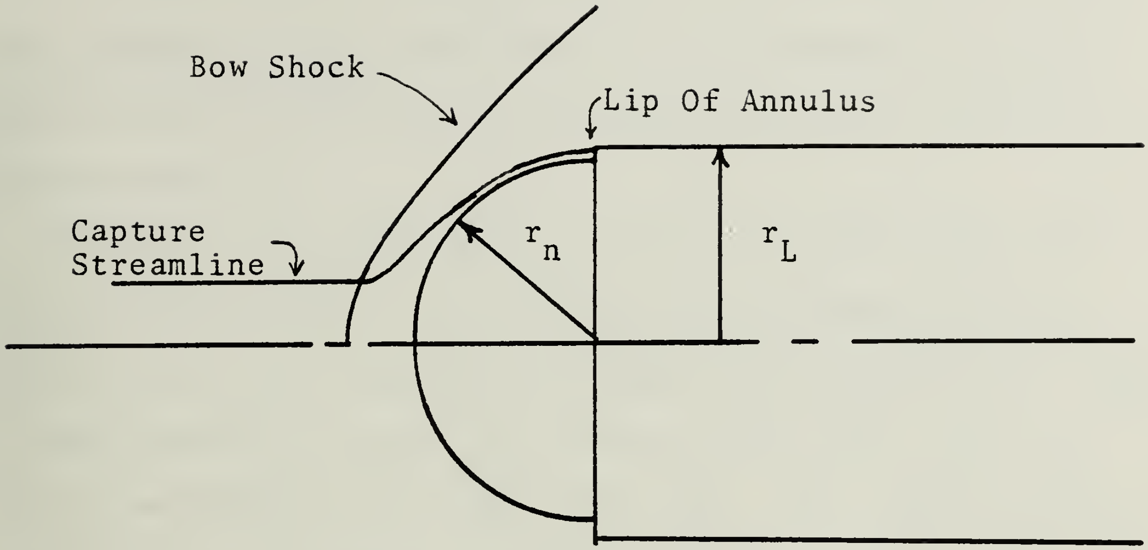

a) $r_L/r_n = 1.1$

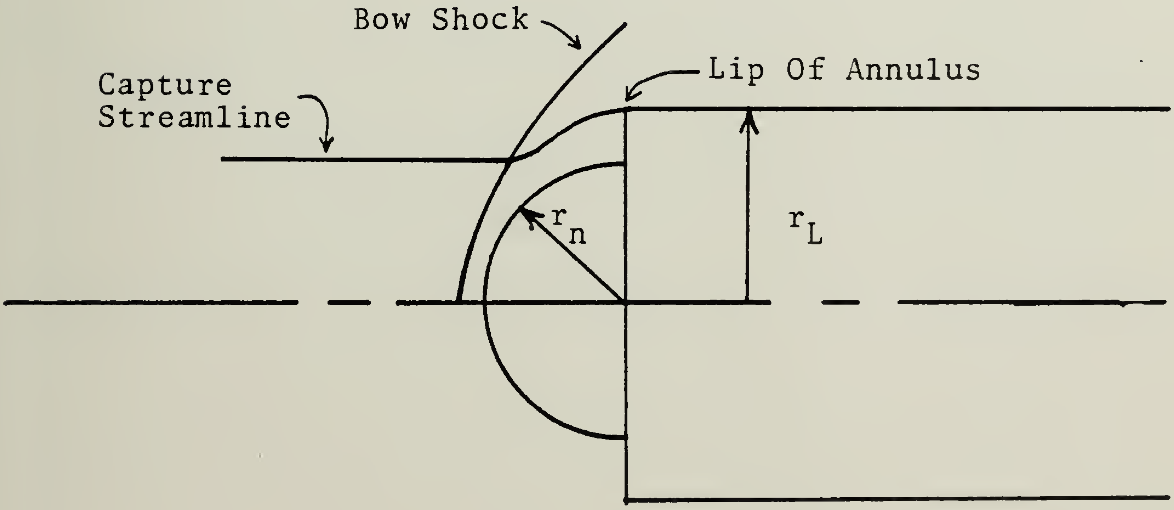

b) $r_L/r_n = 1.4$

Figure IV-7 Bow Shock Wave And Capture Streamtube For r_L/r_n Equal To 1.1 And 1.4

form of a 63% loss of relative detection range must be paid. Lower values of r_L/r_n are unable to be obtained in a thrust equals drag configuration due to high values of additive drag and poor π_d'.

Table IV-1 contrasts ramjets with the spike inlet and two blunt nose inlets. All three ramjets have identical thrust coefficients equal to airframe drag coefficient. Due to large specific thrust, the ramjet with spike inlet requires considerably less mass flow rate. The ramjet with spike inlet has superior specific fuel consumption. Excess thrust is comparable for the three ramjets.

Table VI-1

Comparison Of Spike Inlet Versus Two Blunt Nose Inlets

	Ramjet Using		
Parameter	Spike Inlet	Blunt Nose Inlet	
		Best Ramjet *	Best IR *
Airframe drag coefficient, C_D	0.349	0.349	0.349
Additive drag coefficient, C_{dad}	0	0.018	0.085
Thrust coefficient, C_f	0.349	0.349	0.349
Combustor exit temperature °R, T_{t3}	4122	3284	4422
Mass flow rate, lb_m/sec	9.5	18.3	13.6
Specific Thrust, $lb_f/(lb_m/sec)$	67.2	34.8	46.8
Specific fuel consumption, $(lb_m/hr)/lb_f$	2.02	2.68	3.35
Maximum thrust coefficient C_f, at stoichiometric fuel air ratio	0.505	0.798	0.509
Combustor exit temperature, T_{t3}, °R	5698	5698	5698
Relative detection range	0.33	0.29	0.37

* Best ramjet is obtained for r_L/r_n equal to 1.854 at least for the range of r_L/r_n investigated here. Best IR detection capability occurs for r_L/r_n equal 1.63.

V. CONCLUSIONS

Conversion of the Navy SALGP from a rocket to a ramjet severely degrades detection capability, if an axisymmetric inlet is used. Note the values of 0.33, 0.29, and 0.37 for relative detection range from Table IV-1.

The ramjets with blunt nose inlets suffer in both specific thrust and specific fuel consumption. The poor performance is due to two causes. First, the high value of C_{dad} and second, poor pressure recovery of the inlet leading to poor performance.

Surprisingly, the excess thrust coefficient of ramjets with blunt noses is very competitive with the ramjet with spike inlet.

In view of the foregoing conclusions, pop-out or retractable scoop inlets appear much more attractive in spite of structural constraints and space considerations. Use of an axisymmetric inlet located in the nose of a 5-inch projectile is a severe design compromise.

APPENDIX A

NASA AMES COMPUTER PROGRAM DESCRIPTION

I. INTRODUCTION

Two different computer programs were used to model the flow around the blunt nosed body. The coordinate system used in the thesis and the NASA Ames computer program is shown in Figure II-6.

The first, IMPLCBO, is a modified version of AXI-BLUNT; see Kutler, Chakravarthy, and Lombard [Ref. 9]. Programmed to predict the supersonic flow over a three dimensional body, the algorithm predicts shock shape and location as well as flow parameters at equally spaced interior points between the body and the shock.

The second program, OGIVE, solves for the supersonic flow parameters around a three dimensional wing body configuration; refer to Kutler, Reinhardt, and Warming [Ref. 10]. Originally designed for flow prediction around a delta winged spacecraft, the program will provide flow field parameters at various radii from the centerbody as well as at various locations along the body.

II. PROGRAM DESCRIPTION

The IMPLCBO program uses an unsteady, implicit numerical procedure to determine the supersonic flow around the body. Further program description is contained in Reference 9.

The program output is referenced to various free stream values. These values are shown in Table A-1.

The program utilizes the body configuration and predicted shock points as boundary values and solves the inviscid Euler or Navier-Stokes equations for the interior points, after a coordinate transform.

The different angular relationships at the shock front are shown in Figure A-1.

The OGIVE program utilizes the flow field parameters determined by IMPLCBO, at $\theta = 90°$ and $X = 1.00$, as an initial starting point and determines flow field values along the cylinder body by a finite difference algorithm. The program is further described in Reference 10. The program reference values are tabulated in Table A-1.

The program describes the body shapes by analytical approximations. These approximations consist of coordinate positions and the slope of the body contour as a function of the distance along the body axis.

Table A-1
Reference Values For OGIVE And IMPLCBO Programs

IMPLCBO (region 1)

output variable	reference value
P/PINF	p_∞
RHO/RINF	ρ_∞
U/QINF	$q_\infty = \sqrt{\gamma} M_\infty$; at $M_\infty = 3.0$
V/QINF	$q_\infty = \sqrt{\gamma} M_\infty$; at $M_\infty = 3.0$

OGIVE (region 2)

R	$r_n = 1.0$	
P	$p_{t\infty}$	; $p_\infty / p_{t\infty} = 0.0272237$ at $M_\infty = 3.0$
RHO	$\rho_{t\infty}$	; $\rho_\infty / \rho_{t\infty} = 0.0762263$ at $M_\infty = 3.0$
QINF	$q_\infty = v_\infty / v_m$; $q_\infty = [1 + 5/M_\infty^2]^{1/2}$	
U	q_∞	; Z component of flow velocity
V	q_∞	; R component of flow velocity
W	q_∞	; 0 component of flow velocity
Z	r_n	; length along cylinder body

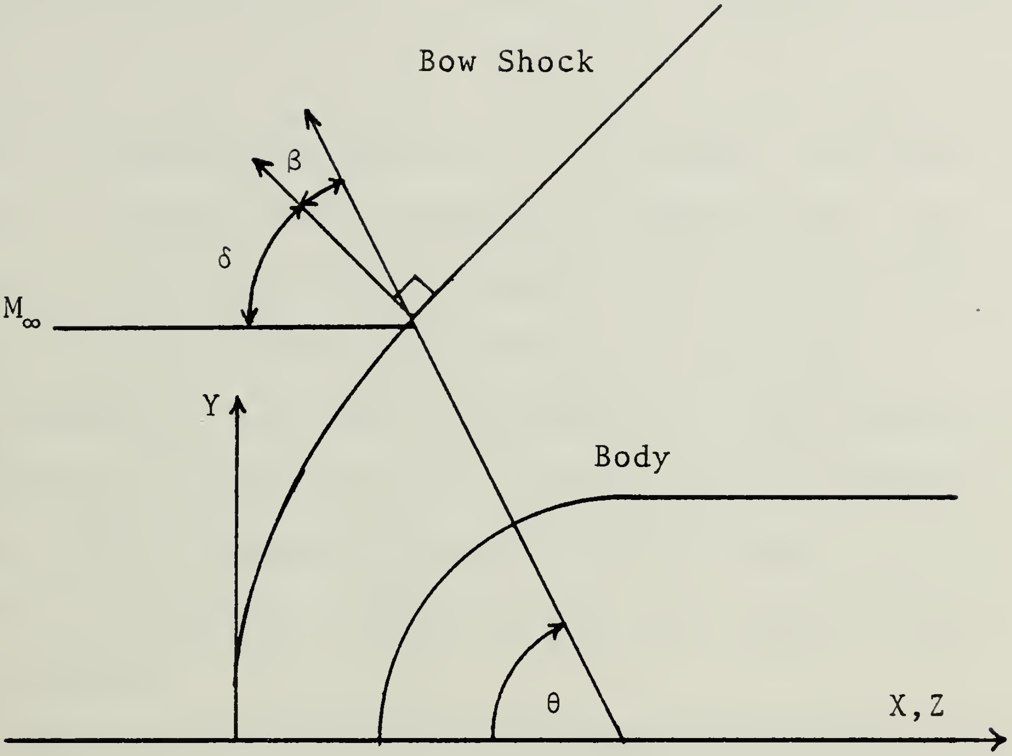

Figure A-1 Angular Relationship At The Shock Front For δ, β, θ

APPENDIX B

MASS CONTINUITY METHOD OF DETERMINING STREAMLINE SHAPE

A computer program has been written for the HP 9830 to calculate the capture streamline. The program is designed to reduce the output data obtained from the NASA Ames computer output and compute the streamtube position at various points in the flow field around the blunt nosed body.

The streamtube position is determined by comparing the mass flow of air entering the bow shock to the integral of mass flux. The streamtube radius at the bow shock, r_s, is determined by comparing the mass flow at the inlet to mass flow at the nose.

The value of the integral in equation (22) or (23) is determined by assuming a linear change in pressure, density and velocity between successive data points. The program interpolates to find the distance from the axis that the streamtube must be to satisfy the mass flow requirements of the inlet. Values of X and Y as shown in Figure II-6 are calculated, and an interpolated pressure is determined. The value of the integral in equation (22) and (23) is calculated using the rectangular method. Equations (22) and (23) are developed in Chapter III of this thesis.

Table B-1

Variables For Capture Streamtube Computer Program

Symbol for HP 9830	Definition
A0	value of integral in equation (22) or (23) between point i and i+1
A7	remaining area between tabulated values
C	squared radius of streamtube at shock front (square inches)
C1	constant for integral when in region I
C2	constant for integral when in region II
F	percentage of distance Y7 is between Y(I) and Y(I+1)
G	dummy variable for area calculation
I	indexing variable
P7	interpolated value of pressure X7,Y7
S7	slope of area curve
W	dummy variable used in calculation of C
Q9	value of Q_∞, equal to $(1+(5/M_\infty))^{-1/2}$
R9	value of $\rho_\infty/\rho_{t\infty}$ at M_∞
S	summation of integral area to the ith point (inches squared)
X7	interpolated value of X, determined from Y7 (inches)
Y7	interpolated value of Y (inches)
Input variables	
A	angular value of data points above projectile centerline (degrees)
I9	number of data points in data file
Z	location of data points in relation to the projectile shoulder. 1= in front of shoulder 2= on the body cylinder

Table B-1 con't

Symbol for HP 9830	Definition
Dimensioned Variables	
G(I)	integral value between i and i+1
L(I)	integral value at ith point
P(I)	pressure ratio at ith point
R(I)	density ratio at ith point
U(I)	component of flow velocity along the body in the Z-direction
V(I)	component of flow velocity along the body in the r direction
Y(I)	distance from the body centerline to the data point

Table B-2 Capture Streamtube Program Listing

```
10 S=A0=0
20 DEG
30 Q9=0.80174
40 R9=1/0.07623
50 PRINT
60 PRINT
70 WRITE (15,80)
80 FORMAT 5X,"I",7X,"P(I)",8X,"R(I)",8X,"Y(I)",8X,"V(I)",8X,"G(I)",7X,"INTEGRAL"
90 PRINT
100 PRINT
110 DISP "INPUT NOSE STREAMTUBE RADIUS";
120 INPUT D
130 C=D↑2
140 READ J,A
150 IF A=90 THEN 170
160 GOTO 180
170 A=89.9999999
180 DIM V[25],Y[25],U[25],R[25],G[25],L[25],P[25]
190 DISP "INPUT Z PRINTOUT 1 Z=1 ...PRINTOUT 2 Z=2";
200 INPUT Z
210 DISP "SURPRESS PRINT, 1=YES";
220 INPUT Y9
230 IF Z=2 THEN 260
240 C1=2
250 GOTO 270
260 C2=2*R9/Q9
270 FOR I=1 TO 21
280 READ P[I],R[I],Y[I],U[I],V[I]
290 NEXT I
300 FOR I=1 TO 21
310 G=V[I]/TAN(A)+U[I]
320 L[I]=G*Y[I]*R[I]
330 IF Y9=1 THEN 360
340 WRITE (15,350)I,P[I],R[I],Y[I],U[I],V[I],G[I]
350 FORMAT F6.0,6F12 4
```

```
360 NEXT 1
370 PRINT
380 PRINT
390 PRINT
400 FOR I=1 TO 20
410 A0=(G[I+1]+G[I])*(Y[I+1]-Y[I])/2
420 S=S+A0
430 L[I]=S
440 IF Z=1 THEN 470
450 IF L[I]>C/C2 THEN 490
460 GOTO 480
470 IF L[I]>C/C1 THEN 490
480 NEXT I
490 IF I=21 THEN 650
500 PRINT "I"I,"L(I)"L[I],"L(I-1)"L[I-1]
510 PRINT "Y(I)"Y[I],"Y(I+1)"Y[I+1]
520 S7=Y[I+1]-Y[I]
530 S7=(G[I+1]-G[I])/S7
540 IF Z=1 THEN 570
550 A7=C/C2-L[I-1]
560 GOTO 580
570 A7=C/C1-L[I-1]
580 W=4*G[I]↑2+(8*A7*S7)
590 W=SQR(W)/(2*S7)
600 W=W-(G[I]/S7)
610 Y7=Y[I]+W
620 X7=Y7/TAN(A)
630 X7=1-X7
640 PRINT
650 PRINT "DATA LINE # IS"J,"STREAMTUBE RADIUS AT NOSE IS"D"INCHES"
660 PRINT "ANGLE FROM BODY CENTERLINE"A
670 IF I=21 THEN 760
```

```
680 PRINT "X7"X7
690 PRINT "Y7"Y7
700 F=((Y7-Y[I])/(Y[I+1]-Y[1]))
710 P7=P[I+1]-P[I]
720 P7=P[I]+(F*P7)
730 PRINT
740 PRINT "INTERPOLATED PRESSURE, P7, IS "P7
750 GOTO 770
760 PRINT "STREAMTUBE POSITION IS HIGHER UP ON PROJECTILE"
770 END
```

APPENDIX C

ADDITIVE DRAG COMPUTATION

The program is designed to calculate the additive drag and coefficient of additive drag for an inlet. The reference area is the projectile base area. The program is written in BASIC for the HP 9830 desk top calculator.

The input data consists of the point position (X and Y) and the static pressure at the point. The three variables X, Y, and p are determined by first running the program described in Appendix B of this thesis.

Equations (27) through (30) used in this calculation are developed in Section III of this thesis.

The computer symbols are listed and defined in Table C-1 and the program listing is in Table C-2.

Table C-1

Variables For Coefficient Of Additive Drag Computer Program

Variables	Definition
A	Reference area (square inches)
C	Coefficient of additive drag between I and I+1 data point (dimensionless)
C1	total coefficient of additive drag (dimensionless)
D	total drag of body
H	distance along body, Z, between data points (inches)
I	counting variable
J	counting variable
P	Ratio of circle circumference to diameter
P1	$\rho_\infty/\rho_{t\infty}$ at input M_∞
R	Distance from centerline, Y (inches)
S	Slant distance between data points (inches)
S1	Surface area of cone between data points (square inches)
W	Incremental drag between data points (lb)
Input variables	
M	Mach number (dimensionless)
I9	Number of data points
Dimensioned variables	
A(I)	Angle of streamtube between data points (degrees)
P(I)	Pressure at Ith data point (dimensionless)
R(I)	Average pressure between data points (dimensionless)
X(I)	X position of Ith data point (inches)
Y(I)	Y position of Ith data point (inches)

Table C-2 Coefficient Of Additive Drag Program Listing

```
10 DIM X[25],Y[25],P[25],A[25],R[25]
20 H=R=W=D=C1=S=S1=0
30 DEG
40 PRINT
50 PRINT
60 P=3.141592654
70 A=(2.5↑2)*P
80 P1=0.02722
90 DISP "INPUT NOSE STREAMTUBE RADIUS";
100 INPUT B
110 DISP "INPUT NOSE CENTERBODY RADIUS";
120 INPUT A5
130 DISP "INPUT MACH NUMBER";
140 INPUT M
150 DISP "INPUT # OF POINTS";
160 INPUT I9
170 PRINT "     ADDITIVE DRAG AND CDAD FOR GIVEN STREAMTUBE DATA"
180 PRINT "     NOSE CENTERBODY RADIUS (INCHES)"B
190 PRINT "     NOSE STREAMTUBE RADIUS (INCHES) "A5
200 PRINT "     MACH # ="M
210 PRINT
220 PRINT
230 FOR I=1 TO I9
240 READ X[I],Y[I],P[I]
250 IF P[I]>1 THEN 270
260 P[I]=P[I]/P1
270 NEXT I
280 WRITE (15,300)
290 PRINT
300 FORMAT 10X,"I",7X,"X(I)",8X,"Y(I)",7X,"P/PINF"
310 FOR I=1 TO I9
320 WRITE (15,330)I,X[I],Y[I],P[I]
330 FORMAT 5X,F6.0,5F12.4
340 NEXT I
350 J=I9-1
```

```
360 PRINT
370 PRINT
380 WRITE (15,390)
390 FORMAT "      PT TO PT",5X,"ANGLE",5X,"P(AVE)",7X,"ADD DRAG",6X,"CDAD"
400 PRINT
410 FOR I=1 TO J
420 R[I]=(P[I+1]+P[I])*0.5
430 H=X[I+1]-X[I]
440 R=Y[I+1]-Y[I]
450 A[I]=ATN(R/H)
460 S=SQR(H↑2+R↑2)
470 S1=P*S*(Y[I+1]+Y[I])
480 W=(R[I]-1)*S1*SIN(A[I])
490 D=W+D
500 C=(2*W)/(1.4*M↑2*A)
510 C=B↑2*C
520 C1=C1+C
530 WRITE (15,540)I,I+1,A[I],R[I],W,C
540 FORMAT 4X,F3.0,2X,F3.0,5X,F6.2,4X,F7.4,6X,F8.5,4X,F8.5
550 NEXT I
560 C1=(A5/B)↑2*C1
570 PRINT
580 PRINT "     REFERENCE AREA IS BASE OF 5 IN. PROJECTILE"
590 PRINT
600 WRITE (15,610)
610 FORMAT "      TOTAL ADDITIVE DRAG",5X,"COEFFICIENT OF ADDITIVE DRAG"
620 WRITE (15,630)D,C1
630 FORMAT 10X,F10.6,1X,"LBF",10X,F12.8
640 END
```

LIST OF REFERENCES

1. Miceli, J.D., Captain, USN, "Navy Guided Projectile", Defense Electronics, v. 11, p. 55-61, July 1979.

2. Toiles, F.W., Gun Propulsion Solid Booster/Ramjet Sustain Preliminary Program Plan, Task area 62766N, Naval Surface Weapons Center, Dahlgren, Virginia, March 1980.

3. Kenroth, G.D. and Anderson, W.R., Ramjet Design Handbook, The Johns Hopkins University Applied Physics Laboratory, CPIA Publication 319, June 1980.

4. United Technologies Chemical Systems Division, Ramjet Technology Review Air Induction System, 2 May 1978.

5. Netzer, D.W., Missile Propulsion Lecture Notes, Lectures presented at Naval Postgraduate School, Monterey, CA, October-December 1980.

6. Fuhs, A.E., Ramjet Propulsion Lecture Notes, Lectures presented at Naval Postgraduate School, Monterey, CA, January-March 1981.

7. Brown, G.L., Propulsion For Ramjet Propelled Guided Projectile for 5"/54, Master's Thesis, Naval Postgraduate School, Monterey, CA, December 1980.

8. White, J.S., Aerodynamics And Control Of A 5-Inch 54 Gun Launched Missile, Master's Thesis, Naval Postgraduate School, Monterey, CA, December 1980.

9. Kutler, P., Chahravarthy, S.R., and Lombard, C.P., Supersonic Flow Over Ablated Nosetips Using An Unsteady Implicit Numerical Procedure, American Institute Of Aeronautics And Astronautics, pp. 78-213, January 1978.

10. Kutler, P., Reinhardt, W.A., and Warming, P.F., Numerical Computation Of Multi-Shocked, Three Dimensional Supersonic Flow Fields With Real Gas Effects, American Institute Of Aeronautics And Astronautics, pp. 72-702, June 1972.

INITIAL DISTRIBUTION LIST

		No. Copies
1.	Defense Technical Information Center Cameron Station Alexandria, Virginia 22314	2
2.	Library, Code 0142 Naval Postgraduate School Monterey, California 93940	2
3.	Mr. Jessie East Naval Surface Weapons Center Dahlgren, Virginia 22448	1
4.	Distinguished Professor A. E. Fuhs, Code 67Fu Department of Aeronautical Engineering Naval Postgraduate School Monterey, California	3
5.	LtCol Jean Reed, USA Defense Advanced Research Projects Agency 1400 Wilson Boulevard Arlington, Virginia 22209	2
6.	Commander, Naval Sea Systems Command Naval Sea Systems Command Headquarters Attn: Code 62YC Washington, D.C. 20360	1
7.	Mr. Conrad Brandts Naval Surface Weapons Center Dahlgren, Virginia 22448	1
8.	Dr. Fred Billig Applied Physics Laboratory Johns Hopkins Road Laurel, Maryland 20810	1
9.	Professor David Netzer, Code 67Nt Naval Postgraduate School Monterey, California 93940	1
10.	Mr. Phillip Morrison Martin Marietta Orlando Division P. O. Box 5837 Orlando, Florida 32855	1

11. Department Chairman, Code 67 1
Department of Aeronautics
Naval Postgraduate School
Monterey, California 93940

12. Mr. Robert V. Ragsac 1
Ramjet Engineering
Chemical Systems Division
United Technologies
P. O. Box 358
Sunnyvale, California 94086

13. Office of Research Administration, Code 012A 1
Naval Postgraduate School
Monterey, California 93940

14. Mr. James O. Bird 1
Atlantic Research Corp.
7511 Wellington Road
Gainesville, Virginia 22065

15. Captain Paul A. Asmus, USN 1
Code SEA62Y
Naval Sea Systems Command Headquarters
Washington, D.C. 20360

16. Lieutenant John F. Moran, USN 2
119 Chapin Road
Hampden, Massachusetts 01036

17. Dr. Paul Kutler 1
202-1
NASA Ames Research Center
aoffett Field, California 94035

Thesis
M8193 Moran 193261
c.1
Performance of an
Oswatisch inlet with
hemispherical center-
body at zero angle
of attack.